Niche theory for within-host parasite dynamics: Analogies to food web modules via feedback loops

Ashwini Ramesh[1*] and Spencer R Hall[1]

[1]Department of Biology, Indiana University, Bloomington, Indiana, USA – 47405

*Corresponding author email: aramesh@iu.edu

Co-author email: sprhall@iu.edu

Mailing address: Biology Building 239, 1001 E 3rd Street, IN 47405 USA

Phone number: + 1 812-855-6009

Statement of authorship: AR and SRH conceptualized the paper. AR performed the analysis and wrote the first draft of the manuscript, and SRH contributed to subsequent revisions.

Data accessibility statement: All Mathematica code will be published in a public repository upon acceptance

Competing Interest: Authors declare no competing interests

ABSTRACT

Why do parasites exhibit a wide dynamical range within their hosts? For instance, why can a parasite only sometimes successfully infect its host? Why do some parasites exhibit large fluctuations? Why do two parasites coinfect, exclude each other, or win only sometimes over another (via priority effects)? For insights, we turn to food webs. An omnivory model (IGP) blueprints one parasite competing with immune cells for host energy (PIE), and a competition model (keystone predation, KP) mirrors a new coinfection model (2PIE). We then draw analogies between models using feedback loops. We translate those loops into the intraspecific direct (DE) and indirect effects (IE) that create various dynamics. Three points arise. First, a prey or parasite can flip between stable and oscillatory coexistence with their enemy with weakening IE and strengthening DE. Second, even with comparable loop structure, a parasite cannot exhibit priority effects seen in IGP due to constraints imposed by production of immune cells. Third, despite simpler loop structure, KP predicts parallel outcomes in the two-parasite model due to comparable structure of interactions between competing victims and their resources and enemies. Hence, food web models offer powerful if imperfect analogies to feedbacks underlying the dynamical repertoire of parasites within hosts.

Key words: intraguild predation, keystone predation, coexistence, coinfection, priority effects, within-host competition, feedback loops, inverse Jacobian matrices

INTRODUCTION

Parasites can show a variety of dynamics within hosts. These within-host dynamics can significantly affect health of individual hosts (Råberg *et al* 2009; Cressler *et al* 2014; Bashey 2015) and alter population-level disease outbreaks (Mideo 2008; Råberg *et al* 2012; Gorisch *et al* 2018). For instance, exposure to parasite propagules often causes infection of some but not all hosts despite seemingly similar starting conditions (Merrill & Cáceres 2018). The success or failure of invasion and persistence of a parasite within a host determines its infection status or even death (Duneau *et al* 2017; Merrill & Cáceres 2018). Once infected, the stability or instability of within-host dynamics can further impact both host health and transmission to others. For instance, periods of high abundance of a cycling gut parasite can both decrease foraging and increase transmission to bee hosts (Otterstatter & Thomson 2006). Similarly, coinfection (*i.e.,* within-host coexistence of parasites) can reduce fecundity of hosts more than single infection (Lohr *et al* 2010). At the between-host scale, coinfection can reduce or increase outbreaks compared to singly infected populations (Clay *et al* 2019; Susi *et al* 2015). Consequently, various dynamics of parasites can arise within hosts, likely mediated by immune systems and nutrient/energy availability (Graham 2008; Cressler *et al* 2014). But which mechanisms determine those dynamics?

To answer this question, two classic food web modules from community ecology provide analogies. In intraguild predation (IGP), an omnivorous predator and its prey compete for a shared resource (Holt & Polis 1997; Verdy & Amarasekare 2010). Similarly, immune cells and a parasite compete for shared energy within a host (Fig. 1A - C; Cressler *et al* 2014). Hence, mechanisms that capture the repertoire of dynamics in IGP (stable coexistence, oscillations, priority effects, exclusion) could also produce those observed in single-parasite studies (Otterstatter & Thomson 2006; Merrill & Cáceres 2018). Additionally, in the diamond-keystone predation (KP) model, two prey species share a resource (exploitative competition) and a predator (apparent competition: Holt *et al.* 1994, Leibold 1996). Similarly, two parasites can compete for a shared resource while facing

71 immune attack (Fig. 1D - F). In such a scenario, the KP model could anticipate the tradeoffs and
72 niche dimensions needed for coexistence, exclusions, and priority effects of coinfecting parasites
73 (Natsopoulou *et al* 2015). The underlying hope, then, is that food web modules might provide apt
74 blueprints, because they share basic consumer-resource structure with their within-host analogues.
75 However, a major complication arises: the enemy is generated differently in food webs vs.
76 within a host (Wodarz 2006). Predators attack and assimilate prey for reproduction into new
77 predators. Immune cells also attack parasites, but they simultaneously require host energy to
78 produce immune cells (Cressler *et al* 2014). These "consumer-resource like" interactions can
79 involve products of immune cells, parasites, and energy. Additionally, hosts can allocate a baseline
80 level of energy straight to immune cells, a pipeline not enjoyed by even omnivorous predators in
81 typical food webs. Therefore, these fundamentals of immune function – even when highly
82 simplified - create more interaction links (Fig. 1). Those additional links might alter feedbacks
83 underpinning the range of stability outcomes (Metcalf *et al* 2020), possibly undermining analogies
84 from food webs or creating new outcomes altogether. Given these issues (Wodarz 2006; Alizon *et*
85 *al* 2008; Fenton & Perkin 2010), how could we usefully compare and contrast stability outcomes
86 in food webs (IGP, KP) to their within-host analogues?
87 We tackle this challenge by using a feedback loop approach. Feedback loops link the
88 strength of consumer-resource interactions to stability (Puccia & Levins 1991). Indeed, feedback
89 loops characterize the biology behind stability and enable comparison of structurally similar but
90 biologically distinct systems. Every n-dimensional system consists of n levels of feedback (F_n).
91 The simplest level of feedback, level 1 (F_1), involves intraspecific direct effects (DE). Here, a
92 small increase of a species impacts its own growth rate – positively or negatively - via interaction
93 with itself and from those directly consuming it. Then, longer loops (from 2 through n dimensions)
94 involve combinations of intra- and inter-specific direct effects (calculated from Jacobian matrices).
95 For instance, in a two-species loop, an increase in a resource's density could increase growth rate

96 of its consumer. Increased density of its consumer, in turn, could then depress growth rate of that
97 resource (hence, binary consumer-resource interactions create negative F_2). With more
98 dimensions, the connections between interactors become more complex and varied, potentially
99 introducing both positive and negative feedbacks. The sign and strength of feedback at all relevant
100 levels, then, governs stability. Additionally, key ratios of those longer loops determine
101 intraspecific indirect effects (IE; developed in Box 1). As we then show, feedback at certain levels,
102 translated into intraspecific direct and indirect effects, determines stability of the interactions.

103 Using intraspecific direct and indirect feedback loops, we first revisit the foundational IGP
104 and KP models. We then apply these loop-based lessons to analogous parasite-immune-energy
105 models (PIE and 2PIE; Fig. 1). To study these analogues, we assume that parasite(s) respond to
106 attack by a common immune system. That assumption surely oversimplifies some examples (*e.g.,*
107 in vertebrates: Ezenwa & Jolles 2011), but it seems like a reasonable place to start for others
108 (Graham 2008; Griffits *et al* 2015; Rynkiewicz *et al* 2015). Additionally, we assume that immune
109 cells and parasites share host energy (a resource, following Griffits *et al* 2015). We then evaluate
110 how host energy and immune system interact to mediate parasite dynamics within hosts (De Roode
111 *et al* 2005; Ezenwa & Jolles 2011; Doublet *et al* 2015).

112 The analysis involves three parts. First, we translate loops into a scheme framed as
113 intraspecific direct and indirect effects (DE and IE). This interpretation works most thoroughly for
114 3D systems (IGP and PIE models), but we extended key ideas to 4D systems (KP and 2PIE
115 models). Second, using these tools, we analyzed stability outcomes for IGP vs. PIE. We find that
116 IGP and PIE share some dynamics (coexistence, stably or via oscillations) due to similar loop
117 structure. However, the nature of the generation of immune cells prevents some outcomes present
118 in IGP (involving two variations on alternate stable states). Third, we find that despite having
119 simpler feedback links, KP anticipates coexistence/coinfection vs. priority effects (or alternate
120 stable states) of competing parasites in 2PIE models. Furthermore, these outcomes arise for

conceptually similar reasons. Specifically, depending on their traits, competing prey or parasites exhibit symmetries (coexistence/coinfection) or asymmetries (priority effects) in ratios describing '*effects on'* their enemies and resources vs. how they are '*affected by*' them. Those (a)symmetries determine the strength of tradeoffs and competitive hierarchies among competitors. They also underpin the sign of feedback at a key level, hence they govern whether parasites experience negative or positive indirect effects. Furthermore, allocation of energy to constitutive immunity enhances negative feedback, thereby shrinking regions of within-host oscillations, coinfection, and parasite burden. Thus, feedback loops, guided by our interpretation schemes, show when and why comparable dynamics arise in these food webs and their within-host analogues. However, we highlight why differences in production of enemies constrain some outcomes within hosts.

METHODS AND RESULTS

Overview of the models

We compare and contrast modules of food web and within-host dynamics. The model with one prey, predator, and resources (intraguild predation, IGP; Holt & Polis 1997; Verdy & Amarasekare 2010) parallels a within-host model of one parasite species, immune cells, and host energy (PIE; modified from Hite & Cressler 2018). Similar, a two prey, predator, resource model (keystone predation, KP; Leibold 1996) parallels one with the new two parasite species, immune cells, and host energy model (2PIE). However, while the food web and within-host modules share similar structure, they create enemies differently. Specifically, predators proliferate via direct consumption of their prey, while immune cells jointly require both parasites and a shared energy. Additionally, the within-host modules include two variants that commonly arise in invertebrate host-parasite systems. In one, only parasites activate production of immune cells (PIE and 2PIE models). In the other, energy is continuously allocated to maintain baseline immune function, even without parasites (PIEc and 2PIEc, constitutive immunity). Despite their differences, we compare

146 across food web and within-host modules using feedback loops. Feedback loops provide a
147 common metric to unpack the biology underlying stability. Jacobian matrices provide the starting
148 point (Box 1, Appendix Section 1). Each of Jacobian terms represents the direct effect of species
149 j on growth rate of species i (J_{ij}), yielding (hereafter) interspecific *positive effects* (black arrow)
150 and *negative effects* (red arrow) and intraspecific *self-limitation* (red curve) or *self-facilitation*
151 (black curve; Box 1, Fig. 1 [not seen here]). As shown below, these terms combine into loops at
152 various levels.
153
154 ***One prey - predator - resource (IGP) | One parasite - immune cells - host energy (PIE & PIEc)***
155 At their heart, both IGP and PIE models hinge on binary consumer-resource like
156 interactions (Fig.2, Table 1). In these interactions, consumers directly benefit while resources
157 suffer direct costs. In IGP, omnivorous predators (P) can consume prey (N_1) and resources (R).
158 An interior equilibrium becomes feasible when each species can maintain positive density ($P^* >$
159 0, $N_1^* > 0$, $R^* > 0$). At IGP's interior, these consumer-resource interactions exert positive effects
160 on the predator but negative ones on prey and resource. Then, prey also indirectly compete with
161 predators for the shared resource. Consumption of resources benefits the prey and harms resources.
162 Finally, chemostat-like renewal imposes self-limitation on resources (Fig. 1A). Similarly, in the
163 within-host models, immune cells (I) "consume" two items, simultaneously killing parasites (N_1)
164 while taking up host energy (E). At PIE's interior, these consumer-resource-like interactions have
165 a positive effect on I and negative on N_1 and E. The parasite competes for this shared energy;
166 consumption of host energy positively effects parasites and negatively effects energy.
167 Additionally, the donor-controlled renewal of host energy imposes self-limitation on energy
168 without baseline allocation ($a_b = 0$; Fig. 1B). Fixed energy allocated to immune cells ($a_b > 0$)
169 creates additional self-limitation on the immune cells in PIEc (Fig. 1C).
170

171 *Intraspecific direct and indirect effects: an approach using feedback (Box 1 and Fig. 2).*

172 To compare stability of these models, we used feedback loops (Box 1). Any *n*-dimensional
173 system can be decomposed into *n* levels of feedback that determine stability of an equilibrium
174 (Box 1, Top Panel). An interior equilibrium can allow stable or unstable coexistence (oscillations)
175 or produce, potentially, alternate stable states (if it is a saddle). As illustrated by and applied to
176 IGP and PIE, the three-dimensional system creates three levels of feedback (Box 1, Fig. 2). For
177 example, level 1 feedback (F_1) is the sum of intraspecific direct effects (Box 1) and is the
178 Jacobian's trace (Appendix Section 1). At the interior of IGP and PIE, the basal resource / energy
179 contributes to the direct effects at the feasible interior (Fig. 2, Appendix Section 2). Self-limitation
180 comes from the chemostat-supplied resource and its consumption; in PIEc, baseline allocation to
181 immunity adds self-limitation (hence negative level 1 feedback [see below but also Appendix
182 Section 1]). Level 2 (F_2) feedback sums up two-species loops (Box 1). In PIE models (Fig. 2), this
183 sum of pairwise consumer resource come from energy-parasite (E-N_1), energy-immune cells (E-
184 I), and parasite-immune cells (N_1-I, with R-N_1, R-P, and N_1-P analogies in IGP, respectively). At
185 the interior, all of these loops contribute to negative feedback. That negative feedback intensifies
186 in PIEc from the product of energy and immune self-limitation. In all 3D models considered here,
187 F_2 is negative at the interior equilibrium (based just on signs alone): level 2 feedback stabilizes.

188 Level 3 feedback (F_3) sums three-species loops. It is also the negative of the determinant
189 of the Jacobian, - |**J**| (Appendix Sections 1, 2). In PIE models, these loops at the interior are (Fig.
190 2, L-R): (i) "*N_1 is eaten*", a negative loop coming from the stabilizing product of the immune-
191 parasite loop and energy self-limitation; (ii) "*starving the enemy*", a positive loop where a small
192 increase in the parasite reduces energy for the immune cells, hence reduces immune attack (i.e.,
193 $\uparrow N_1 \rightarrow \downarrow E \rightarrow \downarrow I \rightarrow \uparrow N_1$); (iii) "*feeding the enemy*", a negative loop where a small increase of the
194 parasite 1 stimulates the immune cells which consume energy that then starves the parasite ($\uparrow N_1 \rightarrow$
195 $\uparrow I \rightarrow \downarrow E \rightarrow \downarrow N_1$). Thus, negative feedback operates when N_1 hurts itself by "feeding" the immune

cells. Similar loops arise in IGP. Finally, in only PIEc, (iv) a negative "N_1 *eats*" loop arises from the stabilizing product of energy consumption by the parasite and immune self-limitation.

Combined, these three levels of feedback determine stability of the interior equilibrium. First, stability requires that each level of feedback is negative (so, $F_1 < 0$, $F_2 < 0$, and $F_3 < 0$). When $F_3 < 0$, the interior is stable; when $F_3 > 0$, it is a saddle. Additionally, stability requires that $F_1 F_2 + F_3 > 0$, or that upper-level feedbacks (F_3) not be too strong relative to lower-level feedback ($F_1 F_2$). All of these conditions have analogies to the Routh-Hurwitz criteria, differing only in sign (Puccia & Levins 1991). Here, we also reframe stability analysis as sums of intraspecific direct effects (F_1, hereafter DE) and of intraspecific indirect effects ($-F_2 / F_3$, the trace of the inverse Jacobian, IE: see Appendix Section 1, Box 1). Written this way, IE is a ratio of the longer loops, where each species interacts with other species in feedback at level 2 (F_2) and level 3 (F_3). It is also the sum of intraspecific indirect effects of each species N_i (lying on tr[$-\mathbf{J}^{-1}$]; Eq. 5):

$$\mathrm{IE} = \mathrm{IE}_{\mathrm{N}_1} + \mathrm{IE}_{\mathrm{N}_2} + \mathrm{IE}_{\mathrm{N}_3} = -F_2/F_3 \qquad \text{(Eq. 5)}$$

The numerator of the intraspecific indirect effects of each species ($\mathrm{IE}_{\mathrm{N}_i}$) corresponds to specific combinations of the reciprocal two-species F_2 loops; the denominator for each species is F_3. For example, in general form, the corresponding indirect effect of N_1, $\mathrm{IE}_{\mathrm{N}_1}$, is the sum of (i) the product of self-limitation of N_2 and N_3 and (ii) pairwise consumer-resource loop of N_2 and N_3, all divided by F_3 (green shading over gray shading, Box 1). Similar expressions can be derived for species 2 ($\mathrm{IE}_{\mathrm{N}_2}$, yellow shading) and 3 ($\mathrm{IE}_{\mathrm{N}_3}$, blue shading). With DE and IE in hand, stability then depends on their sign and the strength of their product. Specifically, *stable coexistence* occurs when direct and indirect effects are negative (DE < 0, IE < 0) and jointly strong (DE x IE > 1; bottom of Box 1, light orange region; equivalent to $F_1 F_2 > -F_3$). *Oscillations* arise when direct and indirect effects are jointly weak (dark orange, DE x IE < 1 for DE < 0, or DE > 0; equivalent to $F_1 F_2 < -F_3$). Finally, *alternate stable states (aka priority effects)* occur with positive indirect effects (IE > 0, *i.e.*, when $F_3 > 0$ for IGP and PIE, given that $F_2 < 0$ for both at their interiors; Box 1, gray region).

Note: we use the terms alternate stable states and priority effects interchangeably. They both denotes how initial densities, even offset in time (*e.g.,* sequential infection), can determine competitive outcomes (depending on whose domain of attraction they move through).

Weakening DE x IE generates oscillations in these models (Fig. 3 and Appendix Section 2)

Assembly of the interior equilibrium: To compare stability outcomes across IGP and PIE models, we created parallel 2D bifurcation diagrams (Fig 3). These diagrams spread gradients of parameter space of an environmental factor, supply of resource (S), and trait space of the focal prey/parasite, feeding rate of N_1 on resource, f_{N_1} (Fig. 3A-C; interpreted with 1D bifurcation diagrams: Fig. 3G-I). The lines within the 2D bifurcation diagram represent shifts in species composition or in dynamics (stable coexistence, oscillations, or alternative stable states; see Appendix Section 2 for full analysis). In IGP (Fig. 3A), when resource supply and feeding rate of prey are too low to meet the minimal resource requirement of either the prey or predator, only R is supported in the system (R, yellow). Increases in S allows R to meet the minimum resource requirement (R^*) of the predator (hence P invades creating the R-P region, green). As feeding rate of prey increases along a fixed resource supply (S = 110), the prey becomes a better competitor for resources, enabling births, $f_{N_1}R^*$, to exceed deaths, $f_{PN_1}\ P^* + m_N$ at the R-P boundary. Hence, the prey can invade; both prey and predator push R^* lower in the R-N_1-P interior (Fig. 3A, Fig. 3G). In this region, R-N_1-P are able to coexist either stably (light orange) or via oscillations (dark orange). On the other hand, as the feeding rate of prey increases at low S (S = 5), prey invade the resource-only boundary (creating the R-N_1 region, blue). The omnivorous predator can then invade this R-N_1 boundary when its birth rate, $e_{PN_1}\ f_{PN_1}\ N_1^* + f_{PR}\ R^*$, exceeds its death rate, m_P. Successful invasion creates stable coexistence (orange; Fig. 3A). Thus, R, R-P, R-N_1, and R-N_1-P equilibria (oscillatory and stable coexistence) are possible.

The within-host PIE model contains some but not all analogous states. The key differences

stem from how hosts produce immune cells. In PIE (Fig. 3B), immune cells only generate with parasites. Hence, a host energy-immune (*E-I*) state, analogous to the *R-P* one, is not possible. Similar to IGP, though, low feeding rate can prevent parasite invasion (creating the *E*-only state [yellow]). With increasing feeding rates (illustrated at S = 500), parasites (N_1) can eventually invade creating E-N_1 space (light blue; Fig. 3H). Although parasites depress E^*, sufficiently high parasite density enables production of immune cells, when the immune system's minimal E N_1 requirement is met (Fig. 3H). Hence, at medium to high feeding rates of parasites, E-N_1-I coexist either stably (light orange) or via oscillations (dark orange). However, at sufficiently high f_{N_1}, parasites compete too strongly: they successfully starve out the immune cells, re-establishing a E-N_1 space (blue). Thus, PIE exhibits only three equilibria: E, E-N_1, and E-N_1-I (oscillations and stable coexistence; Fig. 3B; see Appendix Section 3B for details).

In PIEc, the host always allocates energy to the immune system ($a_b > 0$). This biology eliminates the *E*-alone and E-N_1 region. Instead, immune cells prevent infection (*E-I* space; low f_{N_1}; green) or hosts become infected (E-N_1-I space; higher f_{N_1}; orange). Parasites successfully infect when their births, $(f_{N_1} / e_{N_1E})\, E^*$, exceed their deaths at immune-enhanced, $m_I + f_{IN_1}\, I^*$. Like IGP, at high feeding rates of parasites, the E-N_1-I remains stable (light orange) or oscillates (only at low a_b [Appendix Section 2]). Thus, in PIEc, immune biology eliminates even more states; only *E-I* and E-I-N_1 (oscillations and stable coexistence) remain possible (Fig. 3C).

Stability outcomes: Despite these differences, oscillations arise for similar reasons in the food web and within-host models. As noted in Box 1, oscillations require weakening of the joint product of intraspecific direct effects (DE) and indirect effects (IE). In all three cases, stable coexistence (DE x IE > 1) envelopes oscillatory regions (DE x IE < 1; Fig. 3A-B; Appendix Fig. A2). In IGP, weakening of IE at low feeding rate of the prey, f_{N_1}, triggered oscillations despite strengthening of DE (Fig. 3D). At high f_{N_1}, DE strengthens to regain stability. This general pattern also arises with increasing feeding rate of parasites in the PIE and PIEc models (Fig. 3E-F).

However, DE differed slightly among models (Fig. 3D-F, black, solid lines), where DE is:

IGP: $-a - (f_{N_1}\, Q_{N_1} N_1^* + f_{PR}\, Q_P P^*)$ (Eq. 6A)

PIE: $-r - (f_{N_1}\, N_1^* + e_{IN_1}\, f_{IN_1}\, N_1^* I^*)$ (Eq. 6B)

PIEc: $\underbrace{-r - (f_{N_1}\, N_1^* + e_{IN_1}\, f_{IN_1}\, N_1^* I^*) - a_b}_{DE_E} + \underbrace{\frac{-e_I\, m_I + e_{IN_1} f_{IN_1}\, N_1 E}{e_I}}_{DE_I}$ (Eq. 6C)

Here, either the sum (IGP) or sum and product (PIE) of victim and enemy densities strengthens DE (Eq. 6). Strong enough DE then tips the coexistence equilibrium from oscillations to stability. In IGP the additive increase in predator and prey densities strengthens DE of resources (Eq. 6A). Thus, strengthening of DE restores stability at higher f_{N_1} (Fig. 3D, black, solid line). In the PIE models, however, increase in the (weighted) sum of parasites plus the product of parasite and immune cells strengthens DE of energy at higher f_{N_1} (Eq. 6B-C; Fig. 3E-F, black, solid line).

Constitutive immunity enhanced stability in PIEc models by creating immune self-limitation. This self-limitation generates additional loops featured in both intraspecific direct effects (DE) and indirect (IE; Fig. 2). In PIEc, DE now has two components: DE of energy (DE_E) and DE of immune cells (DE_I; Eq. 6C). The updated DE_E adds fixed energy allocation towards baseline immunity ($-a_b$; Fig. 3F, orange, solid line [DE_E]). DE_I is always negative, too (see Appendix Section 2C). This added immune self-limitation (Fig. 3F, green, solid line [negative DE_I]) further strengthens DE (as shown in Fig. 3E: black, solid line), potentially enough to help to eliminate even the possibility of oscillations in PIEc (eliminated in Fig. 3C; see Appendix Section 2C, Fig. A2). Constitutive immunity also elevates density of immune cells (I^*), lowering parasite burden (N_1^*) while maintaining slightly higher E^* available to hosts for metabolic work (at rE^*; compare Figs. 3H vs. 3I). Hence, constitutive immunity both stabilized dynamics via self-limitation in PIEc (Fig. 2) and reduced parasite burden.

At low feeding rate in both IGP and PIE models, weakening of IE of the prey or parasite triggers oscillations. IE is a ratio of shorter, binary loops (F_2) and longer, three-species loops (F_3)

295 (Fig. 2). In all three models, F_3 became more negative with feeding rate of the prey/parasite, f_{N_1},
296 than did F_2 (as parameterized). That helps explain why the ratio $-F_2/F_3$ (IE) became less negative
297 with increasing f_{N_1} – and hence why weakening IE triggered oscillations (Figs. 2, 3D-F). However,
298 the precise details varied among the models (so it becomes unfruitful to generalize here).
299
300 *Positive feedback leads to alternate stable states in IGP alone (Fig. 4 and Appendix Section 2)*
301 Despite the parallels described above, IGP model can also produce alterative stable states
302 not found in the with-host analogues. In fact, using different parameter values (Fig. 4A; see
303 Appendix Section 2A), a 2D bifurcation diagram shows two forms of alternate stable states in IGP
304 (Fig. 4A; Alt-SS1 [dark grey] and Alt SS-2 [light grey]; see also Verdy & Amarasekare 2010). In
305 these regions, initial densities of species determine competitive outcomes (Fig. 4C, D). The simpler
306 form of alternative stable states (Alt SS – 1; Fig. 4C) yields just the prey (R-N_1) or just the predator
307 (R-P) with the resource. If it held in PIE, analogous outcomes would lead to exclusion of immune
308 cells by parasites (yielding stable infection in the E-N_1 state) or vice versa (yielding immune
309 clearance, a stable E-I), depending on initial parasite dose. However, in PIE, the host cannot
310 generate immune cells without parasites. Consequently, since the E-I state is both biologically and
311 mathematically not feasible, the analogy breaks (Appendix Section 2A). In the other type of
312 alternative stable states in IGP (Alt SS – 2; Fig. 4D), we find either coexistence (R-N_1-P) or a
313 predator-only (R-P) equilibrium, depending on initial conditions (due to two feasible interior
314 equilibria, one of which is a saddle). Such outcomes would resemble a host that became infected
315 (E-N_1-I) or cleared infection (E-I), depending on parasite dose. We could not fine such an outcome
316 in PIEc (see Appendix Section 2C). Hence, despite the qualitatively similar loop structure, IGP
317 offered two scenarios for alternative stable states not present in within-host analogues. Alternative
318 infection states would require some other mechanism to produce positive feedback.
319

Two prey – predator - resource (KP) | Two parasite - immune cells - host energy (2PIE / 2PIEc)

Model Summary (*Fig. 1, Table 2, Appendix Section 3)*

Both keystone predation (KP) and within-host (2PIE) models feature two competitors engaged indirectly via consumer-resource like interactions. In both, consumers directly benefit (positive, black arrow) with direct costs to resources (negative, red circle). In KP, predators (P) can consume two prey (N_i), leading to positive interspecific direct effects for the predator and negative effects on prey (Fig. 1D). The two prey themselves compete for a shared resource (R), creating similar +/- interactions. Additionally, the resource experiences self-limitation at the interior (four species) equilibrium (Fig. 1D). Unlike in IGP, the predator does not consume the resource (i.e., it is not omnivorous). Hence, competitors engage only in apparent and exploitative competition (with P and R, respectively). Similarly, 2PIE and 2PIEc extend the within-host PIE models. Now, two parasites (N_i) compete for host energy but are attacked by immune cells (Fig. 1E-F). During these attacks, immune cells use host energy to proliferate (as described in the PIE models). In 2PIEc, hosts also directly allocate energy to production of immune cells ($a_b > 0$), forging new connections and self-limitation of immune cells (Fig. 1F, Appendix Section 2). Further, *E-I* links introduce additional components of loops not found in KP (e.g., in F_3; Fig 5). Therefore, it might seem that KP provides too simple of a comparison to 2PIE/2PIEc. In fact, 2PIE models best resemble a combination of KP and IGP. Yet, the feedback loops that determine coexistence versus alternate stable states (F_4) of the prey or parasite are qualitatively similar (Fig. 5). The resemblance arises because both the prey and parasite are similarly *effected by* and have *affects on* their resources and their enemy. However, stronger negative feedback at level 3 in 2PIEc will shrink opportunities for coexistence while lowering parasite burden (see below).

Intraspecific direct and indirect effects in the 4D KP and 2PIE model (Fig. 5)

Similar to 3D systems, the sign of intraspecific indirect effects determines coexistence vs. priority effects in 4D systems. But first, in both KP and 2PIE, only self-limitation of the resource or host energy, respectively, contribute to summed intraspecific direct effects (DE; level 1 feedback, F_1; Fig. 5). 2PIEc has additional contributions from the immune self-limitation. Then, summed intraspecific indirect effects (IE) involve a ratio of feedback loops with three species (F_3) and four (F_4; IE = $-F_3/F_4$; Fig 5; Appendix Section 3D). In KP and 2PIE models, F_3 sums the negative consumer-resource loop between each victim and its enemy times self-limitation of the resource (analogous to loop [i] in PIE [Fig. 2]). Then, energy-immune interactions add two sets of additional loops, analogous to positive "*starving the enemy*" and negative "*feeding the enemy*" loops in PIE, but for each parasite (loops [ii] and [iii], respectively). Finally, immune self-limitation in 2PIEc adds two more negative feedback loops (involving $N_i - E$ for each parasite; loops [iv]). At the interior, we find negative F_3 for the interiors evaluated here (algebraically or numerically). Additionally, the sum of loops involving parasite N_2 provide the numerator of the intraspecific indirect effect of N_1 (IE_{N_1}; blue shading), while those involving N_1 provide that of N_2 (IE_{N_2}: purple shading; Fig. 5). Unlike in IGP/ PIE, the intraspecific indirect effect of the enemy and resource now becomes zero. Hence, only the sum of IE_{N_i} determines stability: coexistence occurs when each competitor N_i indirectly decreases its own growth rate.

Importantly, level 4 feedback loops are qualitatively similar across the KP, 2PIE, and 2PIEc models. These loops (from *L-R*) are: (i) a positive *"feeding the enemy"* loop, where a small increase in one parasite stimulates the immune cells which attack the competing parasite, freeing up energy for the first parasite. In a second positive loop, (ii) *"starving the enemy",* a small increase in a parasite reduces resources, hence density of the competing parasite, thereby lowering immune activation, ultimately reducing mortality on the first parasite. Those two positive (destabilizing) loops then push against two negative (stabilizing) loops, (iii and iv) "*N_i is eaten, N_j*

eats". These loops therefore add the stabilizing consumer-resource interactions within which each prey/parasite is enmeshed. For instance, a small increase in parasite *i* creates a negative loop with the immune system while parasite *j* is braked by its loop with the resource. Then, those roles reverse, i.e., parasite *j* is slowed by the immune system and parasite *i* is by the resource. Summed, those two loops (iii and iv) jointly determine the amount of negative feedback in the system at level 4. Combined then, loops (i)-(iv) determine the sign of F_4, the sign of the summed intraspecific indirect effects ($-F_3/F_4$; since $F_3 < 0$: see above), and stability of a feasible interior equilibrium.

In these 4D systems, stability of the interior can also be understood via symmetries or asymmetries in two quantities. These quantities emerge upon rearranging the loops comprising the level 4 feedback (F_4). They reflect ratios of how each prey or parasite has effects on ($-\varepsilon_i$) and is affected by ($-\alpha_i$) their enemies and resources (Fig 5; Eq. 7):

$$F_4 = -J_{N_1E}\, J_{N_2E}\, J_{EN_1}\, J_{EN_2} x \underbrace{\left(\frac{J_{IN_1}}{J_{EN_1}} - \frac{J_{IN_2}}{J_{EN_2}}\right)}_{effects\ on\ (-\varepsilon_i)} x \underbrace{\left(\frac{J_{N_1I}}{J_{N_1E}} - \frac{J_{N_2I}}{J_{N_2E}}\right)}_{affected\ by\ (-\alpha_i)} \qquad \text{(Eq. 7)}$$

where J_{ij} are interspecific direct effects (Jacobians) of species *j* on species *i*, $\varepsilon_I = -J_{IN_1}/J_{EN_1}$, $\alpha_I = -J_{N_1I}/J_{N_1E}$, *etc.* Stability hinges on (a)symmetry of these ratios. As described elsewhere (Appendix Sections 3A, B), the difference in *affected by* ratios ensures a tradeoff in traits influencing resource and apparent competition that permits coexistence. If N_1 is the superior resource competitor without the enemy, then $\alpha_1 > \alpha_2$ ensures N_2 is sufficiently resistant to attack. The difference in *effects on* ratios then determines arrangements of competitive hierarchies with enemies (involving exploitative [resource, energy] and apparent [predator, immune] competition). Coexistence occurs with symmetry in these ratios (i.e., if $\alpha_1 > \alpha_2$ if $\varepsilon_1 > \varepsilon_2$), guaranteeing that net negative feedbacks dominate ($F_4 < 0$). In contrast, asymmetry in these ratios, (e.g., $\alpha_1 > \alpha_2$ still but now $\varepsilon_1 < \varepsilon_2$) leads to net positive feedback ($F_4 > 0$), triggering alternate stable states.

394 *Coexistence (coinfection) and alternate stable states (priority effects) in KP & 2PIE (Fig. 6 and*
395 *Appendix Section 3)*

396 Despite differences in biology, KP and 2PIE models share similar four species feedback loops,
397 hence qualitatively similar outcomes for stability of the interior equilibrium. That similarity
398 becomes readily apparent in 2D bifurcation diagrams for each model in parameter space of supply
399 point (S) – N_1's feeding rate on resources (f_{N_1}). In KP (Fig. 6A), at low S-f_{N_1}, only the resource is
400 supported in the system (R, yellow). Increased feeding rate at low resource supply enables prey N_1
401 to meet its minimum resource requirement (R-N_1; light blue). As S increases, the minimum prey
402 requirement of the predator is met (its N_1^*) allowing predators to invade (R-N_1-P; dark blue). Then,
403 the more resistant N_2 can invade when the R-N_1-P food chain provides enough resources, given
404 predator density (mortality). This invasion enables four species coexistence (R-N_1-N_2-P; light
405 orange). Similar assembly rules apply for invasion of N_2 when feeding rate of N_1 stays low enough
406 to grant N_2 competitive superiority ($R_2^* < R_1^*$). With increasing S, first N_2 invades (R-N_2 space;
407 light purple), then the predator does (R-N_2-P: dark purple). A less typical assembly arises at lower
408 S ($S = 1$) but with increasing f_{N_1}. Here, N_1 and P simultaneously invade creating the jump from 2
409 (R-N_2) to 4 (R-N_1-N_2-P) dimensional stability (see Appendix Section 3C for details). Overall,
410 similar transitions appear in 2PIE models. Like KP, the possible states in 2PIE models are energy
411 alone (E), just one parasite (E-N_i), addition of immune cells (E-N_i-I), or an interior (E-N_1-N_2-I; Fig.
412 6B). However, since hosts always allocate energy to immune cells, they are always present in
413 2PIEc. Hence, 2PIEc only has E-I, E-I-N_i, and E-N_1-N_2-I states (but not E or E-N_i; Fig. 6C).

414 In all three models, low or high combinations of supply point (S) and feeding rate (f_{N_1}), create
415 (a)symmetry in *effects on* and *affected by* ratios that, in turn, generate coexistence or alternate
416 stable states for a feasible interior. We assume N_1 competes superiorly for energy without immune
417 cells but is sufficiently more vulnerable to immune attack (enabling $\alpha_1 > \alpha_2$). In the coexistence
418 region (i.e., at lower f_{N_1}- S), N_1 is the superior apparent competitor while more resistant N_2 is the

superior resource competitor (see Appendix Section 3A,B for details and proof). Such a switch in competitive hierarchy means N_1 exerts stronger effects on immune cells relative to energy ($\varepsilon_1 > \varepsilon_2$; Eq. 7). It also produces a symmetry in ratios that generates net negative feedback ($F_4 < 0$) and negative intraspecific indirect effects of the competitors ($IE_i < 0$) enabling coexistence (coinfection; 6D-F). However, high f_{N_1}- S produces an asymmetry: N_2 now is the superior apparent competitor, and it has stronger effects on immune cells relative to energy ($\varepsilon_1 < \varepsilon_2$) while N_1 is the superior resource competitor. This asymmetry in ratios generates net positive feedback ($F_4 > 0$) triggering alternate stable states (or priority effects; Appendix Section 3A,B). Hence, this interior saddle separates dominance by one or the other parasite (or prey). Furthermore, intraspecific indirect effects are both positive ($IE_{N_i}>0$): each competitor now benefits itself through the feedback loops. With even higher f_{N_1}, N_2 becomes excluded in all three models (Fig. 6G-I). Notice also how, at the border of that exclusion from the coexistence region, IE_{N_2} becomes extremely strong (infinitely negative, since $F_4 = 0$; Fig. 6D-F). In other words, the excluded species suffers extremely strong negative intraspecific indirect effects (i.e., $IE_{N_2} \rightarrow -\infty$).

The 2PIEc model modifies the patterns in 2PIE in qualitative and quantitative ways. Qualitatively, the range of outcomes in S-f_{N_1} space simplifies (as in PIEc: Fig. 4C). Since baseline allocation guarantees positive density of immune cells, there are no E or E-N_i regions like in 2PIE (Fig. 6B vs. 6C). Quantitatively, in the co-infection region, constitutive immunity strengthens intraspecific indirect effects (because of the added negative feedback in the F_3 loops, the numerator of IE of each species [Fig. 5]). Stronger IE, in turn, narrows the parameter space permitting coexistence. Constitutive immunity also elevates density of immune cells (I^*), lowering parasite burden ($N_1^* + N_2^*$) while maintaining slightly higher E^* (allocated at rE^*) for other metabolic work (compare Figs. 6H vs. 6I). Hence, constitutive immunity adds to F_3 loop structure of 2PIEc (Fig. 5). That addition squeezes coinfection space while reducing parasite load relative to 2PIE.

DISCUSSION

What within-host factors determine parasite dynamics? To answer this question, we compare two classic food web modules, intraguild predation (IGP) and keystone predation (KP), to their within-host analogues (PIE and 2PIE). On the one hand, the comparison seems apt. Both prey and parasite consume a shared resource while facing mortality from an enemy (predator or immune cell). On the other hand, predator and immune cells are produced rather differently. For instance, predators can eat only prey or the resource or both (in IGP). In contrast, induced proliferation of immune cells requires both energy and parasites simultaneously. Furthermore, hosts can allocate energy to immunity constitutively (a pipeline uncommon to food webs). Given these similarities and differences, we analyze stability of equilibria produced by each model using feedback loops. In particular, we interpret loops as direct and indirect intraspecific effects, and we show how their sign and strength govern stability outcomes (Box 1). With these tools, we make three points. First, both IGP and PIE systems predict stable coexistence / infection or oscillations due to similar shifts in direct and indirect effects (Fig. 2-3). Second, that enemy-generation difference eliminates alternative stable states (priority effects) seen in IGP – the PIE models cannot produce them without inclusion of some other mechanisms (Fig. 4). Third, despite that KP is structurally simpler than 2PIE models, competing prey and parasites coexist (co-infect) or show priority effects for essentially the same reasons (Fig. 5-6). The outcomes hinge on the sum of similar four-dimensional loops that generate positive and negative feedback. We show how those loops, in turn, translate into parallel symmetries (stabilizing) or asymmetries in *effects on* and *affected by* ratios of the two competitors. Overall, food web models offer powerful if imperfect analogies to feedbacks underlying the dynamical repertoire of parasites within hosts.

Feedback loops enabled biologically meaningful comparisons of the stabilizing and destabilizing forces in the models analysed here. Traditionally, one evaluates (local) stability using Routh-Hurwitz criteria (Routh 1877; Hurwitz 1895). By rearranging these criteria, we unpack the

469 biology of the feedback loops underlying stability (Box 1; Puccia & Levins 1991; Novak *et al*
470 2016). These loops can involve shorter, direct effects (DE), where increases in intraspecific density
471 leads to self-limitation (negative feedback) or facilitation (positive). Longer loops involve chains
472 of connected interactions – here, between two (e.g., binary consumer-resource), three, or four
473 species (Puccia & Levins 1991). We show that certain ratios of these loops at different feedback
474 levels, in turn, correspond to intraspecific indirect effects (IE – falling along the trace of the inverse
475 Jacobian matrix evaluated at the equilibrium; Box 1). Furthermore, we illustrate how negative IE
476 leads to coexistence (stable or oscillatory [in 3D systems]), and positive IE can produce alternative
477 stable states. In 3D systems, that transition from stability to oscillations involves weakening of DE
478 x IE. Such weakening occurs when feedback at longer loops becomes too strong relative to those
479 at shorter loops. With that framework in mind, the loops then facilitated comparison between
480 structurally similar but biologically distinct systems (Novak *et al* 2016), *e.g.,* food web and within-
481 host modules. Indeed, loops can reveal the biology obscured or overlooked in stability analysis.
482
483 ***Single infection dynamics***
484 This loop-based approach to stability analysis revealed that single prey and parasite can persist
485 – stably or via oscillations – with their resource and enemy for similar reasons. Generally speaking,
486 like in IGP, coexistence in PIE requires summed negative intraspecific indirect effects (IE). Like
487 in IGP, weakening of IE ($-F_2/F_3$) triggers oscillations in PIE (due to weakening of F_3 relative to
488 F_2; Fig. 3D-E). Yet, either the sum (IGP) or sum and product (PIE) of victim and enemy densities
489 strengthens intraspecific direct effects (DE). Strong enough DE then tips the coexistence
490 equilibrium from oscillations to stability. Those oscillations matter because they create boom-bust
491 cycles of parasite and immune response that can harm hosts (Otterstatter & Thomson 2006; Childs
492 & Buckee 2015). For instance, these oscillations produce rapid ramp up or down of immune
493 function that can stress host physiology (exacting e.g., oxidative damage, cellular senescence),

494 making them sicker (Costantini & Mølle 2009). However, in hosts with high constitutive immunity
495 (PIEc), the strengthening of DE by immune-self limitation can prevent oscillations, potentially
496 reducing immune damage to host. Additionally, constitutive immunity can improve host health by
497 lowering parasite burden while maintaining higher energy for other metabolic work.

498 Despite similarities in loop structure, alternate stable states emerge in IGP but not PIE models.
499 The reason for this discrepancy hinges on production of the enemies. In principle, when each prey
500 / parasite *"starves the enemy"* enough, the resulting positive feedback through the three species
501 might trigger alternative stable states (alt SS; Fig. 2). In fact, IGP with a semi-chemostat like
502 resource produces two types of them (Verdy & Amarasekare 2010). In the simpler, more typical
503 one, either the prey or the predator dominates. In the other less common one, predator and prey
504 coexist or the prey is excluded (Fig. 4A). If they existed, such alt SS in PIE models might explain
505 why large infectious doses overwhelm immune clearance, leading to infection (yielding stable E-
506 N_1 or E-N_1-I states), while small doses can be cleared by the immune system (in a stable E-I state;
507 as seen in experiments, e.g., Merrill & Cáceres 2018). Yet, we found no such alt SS in PIE or PIEc
508 as formulated (nor did it arise in a similar model with another representation of immune
509 functioning: Greenspoon *et al.* 2018). Hence, some other mechanism is needed to generate alt SS
510 within hosts (e.g., effects of parasites on within-host resource supply points: van Leeuwan *et al.*
511 2019). In the future, such mechanisms could be added to the PIE/PIEc framework. However, they
512 would likely break the straightforward food web analogues that we strove for here.

513

514 ***Coinfection dynamics***

515 In contrast, KP and 2PIE models produced either coexistence or priority effects of competitors
516 for similar reasons. At first glance, such parallels might seem surprising since KP more simply
517 connects species engaged in resource and apparent competition. In contrast, 2PIE has more
518 complex loop structure (created by those omnivory-like I-E connections). Despite these structural

519 differences, both models share qualitatively identical four species loops that govern stability (Fig.
520 5). We translated the net sum of those positive and negative loops into differences in *effects on*
521 and *affected by* ratios for each competitor. Those ratios then lay out conditions for successful
522 coinfection *vs.* alternative stable states (priority effects). First, either case requires a sufficient
523 tradeoff. If one species competes superiorly for host energy, the other must better resist immune
524 attack. Such a tradeoff anchors a directionality of the *affected by* ratio (immune to energy) between
525 competing parasites. Coinfection (and coexistence more broadly), then, requires a symmetry: the
526 parasite with greater *affected by* ratio must also have the greater *effects on* ratio (Fig. 5). Those
527 conditions arise when the superior energy competitor without immune cells (i.e., the one with
528 lower minimal energy needs) becomes the superior apparent competitor with them (i.e., the one
529 that supports and withstands the highest immune density). Meanwhile, the more resistant parasite
530 becomes the best energy competitor. If true, each parasite indirectly inhibits its own growth and
531 facilitates its competitor. Coinfection ensues due to net negative feedback. In contrast, if one
532 parasite always competes superiorly for energy while the superior apparent competitor enjoys
533 resistance, asymmetry in these ratios ensues. That asymmetry means each competitor indirectly
534 facilitates its own growth and slows its competitor, either by *"feeding the immune cells"* that attack
535 the competitor (freeing up energy), or by *"starving the immune cells"* via starving the competitor
536 (Fig. 5). When strong enough, such interactions ensure priority effects via net positive feedbacks.
537 These new within-host competition models can also guide future coinfection experiments.
538 First, the competition models focus attention on traits and mechanism. Traditional coinfection
539 experiments alter initial densities / order of arrival of parasites within a host (Lohr *et al* 2010;
540 Natsopoulou *et al* 2015; *reviewed in* Karvonen *et al* 2019). Then, mechanism is inferred from
541 pattern. Alternatively, with 2PIE-like models in hand now, experimenters can directly measure
542 and/or fit key host-parasite traits that produce within-host dynamics. Second, they highlight how
543 multiple niche dimensions govern competitive outcomes within hosts. Some recent empirical

544 studies emphasized immune- (Ezenwa *et al* 2010; Halliday *et al* 2018) or resource-mediated
545 (Budischak *et al* 2018) competition within hosts. Yet, competition along a single niche dimension
546 predicts only competitive exclusion (*sensu stricto*). Instead, measurements of both immune and
547 energetic niche dimensions together (like in Budischak *et al* 2015) could evaluate the entire range
548 of outcomes anticipated by 2PIE. Third, the bifurcation maps here suggest joint manipulation of
549 resource supply to hosts and parasite traits, perhaps leveraging genetic variation in traits among
550 parasite strains. Such manipulations could then capture a whole array of within-host competitive
551 outcomes (Budischak *et al* 2018) or explain increasing parasite burden along a resource gradient
552 (Wale *et al* 2017). Finally, our model predicts that allocation to constitutive immunity strengthens
553 indirect effects, squeezing parameter space allowing coinfection and reducing parasite burden. One
554 could test such predictions using strains with immune knockouts (like in Chen *et al* 2020) or host
555 genotypes differing in allocation (Fuess *et al* 2020).
556
557 ***Future directions and conclusion***
558 This within-host parasite framework could become expanded in the future. First, models could
559 add niche dimensions. For instance, parasites might compete for multiple within-host resources
560 (Budishack *et al* 2015; Ezenwa 2021) and/or face multiple immune defenses (Jolles *et al* 2008;
561 Ezenwa & Jolles 2011). These additional dimensions parallel food webs with multiple resources
562 and predators (necessitating statements of clear assumptions about specialist vs. generalist
563 consumption, different possible tradeoffs, etc.: Hulot & Loreau 2006). These niche dimensions
564 might expand conditions promoting coinfection or priority effects (Graham 2008; Rynkiewicz *et*
565 *al* 2015). Second, other mechanisms like relative non-linearities (Armstrong & McGehee 1980),
566 competitive intransitivity (May & Leonard 1975), or other variation-based mechanisms (Chesson
567 2000) may predict successful coexistence in our within-host framework. For example, since PIE
568 can oscillate, two parasites might coexist via oscillations (relative non-linearities). Similarly,

569 multiple parasites competing intransitively for two or more resources might coexist (Huisman &
570 Weissing 2001). Finally, environmental variation could alter key within-host traits (*e.g.,*
571 temperature fluctuations can modulate host immunity and parasite attack rates [Scharsack *et al*
572 2016]). Such intersections of environment with trait plasticity might then alter or enhance
573 opportunities for parasite coexistence (Chesson 2000). Finally, the direct (DE) vs. indirect effect
574 (IE) approach to predicting oscillations may have limits. Perhaps theoreticians can extend it
575 beyond three to four or more dimensions. Together, these expansions would extend mechanistic
576 models of within-host dynamics and produce insight into disease and coexistence alike.

577 In this study, we gleaned insights for within-host parasite dynamics using food web modules
578 and feedback loops. Feedback loops enabled comparison of stability outcomes in structurally
579 similar but biological distinct systems. For instance, similarity in loop structure in IGP and PIE
580 successfully predicted single prey / parasite persistence either stably or via oscillations. Yet,
581 despite these structural similarities, differences in generation of enemies (predator vs. immune
582 cells) prevented IGP's two alternate stable states from arising in PIE. In contrast, despite
583 omnivory-like *I-E* connections in 2PIE, competing prey or parasites coexist (coinfect) or show
584 priority effects like in KP. Those outcomes arose because competitors within hosts or in food webs
585 engage in structurally similar resource and apparent competition. Such comparable structure meant
586 that symmetries in *effects on* and *affected by* ratios (involving the enemy and resource) determined
587 stability of competition. Hence, dynamical forces governing stability in food-webs can mirror
588 those within hosts. Such insights can guide more predictive experiments at the within-host scale
589 but also better population-level models. For instance, fluctuation in food supply could shift
590 competitive outcomes within hosts that then shifts multi-parasite outbreaks at the population scale.
591 Hence, further development of resource and immune-explicit frameworks can only enhance
592 predictive insight into host health and disease outbreaks alike.
593

ACKNOWLEDGMENTS

AR was supported by the Department of Biology, Indiana University – Bloomington. The study was supported in part by NSF DEB (grant 1655656). We thank F. Bashey-Visser, C.M Lively, and members of the Hall lab for their valuable feedback.

619 **REFERENCES**

620 Alizon, S., & van Baalen, M. (2008). Multiple infections, immune dynamics, and the evolution
621 of virulence. The American Naturalist, 172(4), E150-E168.
622
623 Armstrong, R. A., & McGehee, R. (1980). Competitive exclusion. The American Naturalist,
624 115(2), 151-170.
625
626 Bashey, F. (2015). Within-host competitive interactions as a mechanism for the maintenance of
627 parasite diversity. Philosophical Transactions of the Royal Society B: Biological Sciences,
628 370(1675), 20140301.
629
630 Budischak, S. A., Wiria, A. E., Hamid, F., Wammes, L. J., Kaisar, M. M., van Lieshout, L., ... &
631 Graham, A. L. (2018). Competing for blood: the ecology of parasite resource competition in
632 human malaria–helminth co-infections. *Ecology letters*, *21*(4), 536-545.
633
634 Budischak, S. A., Sakamoto, K., Megow, L. C., Cummings, K. R., Urban Jr, J. F., & Ezenwa, V.
635 O. (2015). Resource limitation alters the consequences of co-infection for both hosts and
636 parasites. International Journal for Parasitology, 45(7), 455-463.
637
638 Chesson, P. (2000). Mechanisms of maintenance of species diversity. Annual review of Ecology
639 and Systematics, 31(1), 343-366.
640
641 Chen, C. C., Louie, S., McCormick, B., Walker, W. A., & Shi, H. N. (2005). Concurrent
642 infection with an intestinal helminth parasite impairs host resistance to enteric Citrobacter

643 rodentium and enhances Citrobacter-induced colitis in mice. *Infection and immunity*, *73*(9),
644 5468-5481.
645
646 Childs, L. M., & Buckee, C. O. (2015). Dissecting the determinants of malaria chronicity: why
647 within-host models struggle to reproduce infection dynamics. *Journal of The Royal Society*
648 *Interface*, *12*(104), 20141379.
649
650 Clay, P. A., Cortez, M. H., Duffy, M. A., & Rudolf, V. H. (2019). Priority effects within
651 coinfected hosts can drive unexpected population-scale patterns of parasite prevalence. *Oikos*,
652 *128*(4), 571-583.
653
654 Costantini, D., & Møller, A. P. (2009). Does immune response cause oxidative stress in birds? A
655 meta-analysis. Comparative Biochemistry and Physiology Part A: Molecular & Integrative
656 Physiology, 153(3), 339-344.
657
658 Cressler, C. E., Nelson, W. A., Day, T., & McCauley, E. (2014). Disentangling the interaction
659 among host resources, the immune system and pathogens. Ecology letters, 17(3), 284-293.
660
661 De Roode, J. C., Helinski, M. E., Anwar, M. A., & Read, A. F. (2005). Dynamics of multiple
662 infection and within-host competition in genetically diverse malaria infections. *The American*
663 *Naturalist*, *166*(5), 531-542.
664
665 Doublet, V., Natsopoulou, M. E., Zschiesche, L., & Paxton, R. J. (2015). Within-host
666 competition among the honey bees pathogens Nosema ceranae and Deformed wing virus is
667 asymmetric and to the disadvantage of the virus. *Journal of invertebrate pathology*, *124*, 31-34.

Duneau, D., Ferdy, J. B., Revah, J., Kondolf, H., Ortiz, G. A., Lazzaro, B. P., & Buchon, N. (2017). Stochastic variation in the initial phase of bacterial infection predicts the probability of survival in D. melanogaster. *Elife*, *6*, e28298.

Ezenwa, V. O. (2021). Co-infection and nutrition: integrating ecological and epidemiological perspectives. In *Nutrition and Infectious Diseases* (pp. 411-428). Humana, Cham.

Ezenwa, V. O., & Jolles, A. E. (2011). From host immunity to pathogen invasion: the effects of helminth coinfection on the dynamics of microparasites. *Integrative and comparative biology*, *51*(4), 540-551.

Ezenwa, V. O., Etienne, R. S., Luikart, G., Beja-Pereira, A., & Jolles, A. E. (2010). Hidden consequences of living in a wormy world: nematode-induced immune suppression facilitates tuberculosis invasion in African buffalo. *The American Naturalist*, *176*(5), 613-624.

Fenton, A., & Perkins, S. E. (2010). Applying predator-prey theory to modelling immune-mediated, within-host interspecific parasite interactions. *Parasitology*, *137*(6), 1027-1038.

Fuess, L. E., Weber, J. N., den Haan, S., Steinel, N. C., Shim, K. C., & Bolnick, D. I. (2020). A test of the Baldwin Effect: Differences in both constitutive expression and inducible responses to parasites underlie variation in host response to a parasite. *bioRxiv*.

Gorsich, E. E., Etienne, R. S., Medlock, J., Beechler, B. R., Spaan, J. M., Spaan, R. S., ... & Jolles, A. E. (2018). Opposite outcomes of coinfection at individual and population scales. *Proceedings of the National Academy of Sciences*, *115*(29), 7545-7550.

Graham, A. L. (2008). Ecological rules governing helminth–microparasite coinfection. Proceedings of the National Academy of Sciences, 105(2), 566-570.

Greenspoon, P. B., Banton, S., & Mideo, N. (2018). Immune system handling time may alter the outcome of competition between pathogens and the immune system. *Journal of theoretical biology*, *447*, 25-31.

Griffiths, E. C., Fairlie-Clarke, K., Allen, J. E., Metcalf, C. J. E., & Graham, A. L. (2015). Bottom-up regulation of malaria population dynamics in mice co-infected with lung-migratory nematodes. Ecology letters, 18(12), 1387-1396.

Halliday, F. W., Umbanhowar, J., & Mitchell, C. E. (2018). A host immune hormone modifies parasite species interactions and epidemics: insights from a field manipulation. *Proceedings of the Royal Society B*, *285*(1890), 20182075.

Hite, J. L., & Cressler, C. E. (2018). Resource-driven changes to host population stability alter the evolution of virulence and transmission. Philosophical Transactions of the Royal Society B: Biological Sciences, 373(1745), 20170087.

Holt, R. D., & Polis, G. A. (1997). A theoretical framework for intraguild predation. The American Naturalist, 149(4), 745-764.

Holt, R. D., Grover, J., & Tilman, D. (1994). Simple rules for interspecific dominance in systems with exploitative and apparent competition. The American Naturalist, 144(5), 741-771.

Hulot, F. D., & Loreau, M. (2006). Nutrient-limited food webs with up to three trophic levels: feasibility, stability, assembly rules, and effects of nutrient enrichment. Theoretical Population Biology, 69(1), 48-66.

Hurwitz, A. (1895). On the conditions under which an equation has only roots with negative real parts. *Math. Ann.* 46, 273-284 (1895)

Jolles, A. E., Ezenwa, V. O., Etienne, R. S., Turner, W. C., & Olff, H. (2008). Interactions between macroparasites and microparasites drive infection patterns in free-ranging African buffalo. *Ecology*, *89*(8), 2239-2250.

Huisman, J., & Weissing, F. J. (2001). Fundamental unpredictability in multispecies competition. *The American Naturalist*, *157*(5), 488-494.

Karvonen, A., Jokela, J., & Laine, A. L. (2019). Importance of sequence and timing in parasite coinfections. *Trends in parasitology*, *35*(2), 109-118.

Leibold, M. A. (1996). A graphical model of keystone predators in food webs: trophic regulation of abundance, incidence, and diversity patterns in communities. The American Naturalist, 147(5), 784-812.

Lohr, J. N., Yin, M., & Wolinska, J. (2010). Prior residency does not always pay off–co-infections in Daphnia. Parasitology.

May, R. M., & Leonard, W. J. (1975). Nonlinear aspects of competition between three species.

SIAM journal on applied mathematics, 29(2), 243-253.

Merrill, T. E. S., & Cáceres, C. E. (2018). Within-host complexity of a plankton-parasite interaction. Ecology, 99(12), 2864-2867.

Metcalf, C. J. E., Grenfell, B. T., & Graham, A. L. (2020). Disentangling the dynamical underpinnings of differences in SARS-CoV-2 pathology using within-host ecological models. *PLoS pathogens*, *16*(12), e1009105.

Mideo, N., Alizon, S., & Day, T. (2008). Linking within-and between-host dynamics in the evolutionary epidemiology of infectious diseases. Trends in ecology & evolution, 23(9), 511-517.

Natsopoulou, M. E., McMahon, D. P., Doublet, V., Bryden, J., & Paxton, R. J. (2015). Interspecific competition in honeybee intracellular gut parasites is asymmetric and favours the spread of an emerging infectious disease. *Proceedings of the Royal Society B: Biological Sciences*, *282*(1798), 20141896.

Novak, M., Yeakel, J. D., Noble, A. E., Doak, D. F., Emmerson, M., Estes, J. A., ... & Wootton, J. T. (2016). Characterizing species interactions to understand press perturbations: what is the community matrix?. *Annual Review of Ecology, Evolution, and Systematics*, *47*, 409-432.

Otterstatter, M. C., & Thomson, J. D. (2006). Within-host dynamics of an intestinal pathogen of bumble bees. *Parasitology*, *133*(6), 749.

Puccia, C. J., & Levins, R. (1991). Qualitative modeling in ecology: loop analysis, signed digraphs, and time averaging. In Qualitative simulation modeling and analysis (pp. 119-143). Springer, New York, NY.

Råberg, L. (2012). Infection intensity and infectivity of the tick-borne pathogen Borrelia afzelii. *Journal of evolutionary biology*, *25*(7), 1448-1453.

Råberg, L., Graham, A. L., & Read, A. F. (2009). Decomposing health: tolerance and resistance to parasites in animals. *Philosophical Transactions of the Royal Society B: Biological Sciences*, *364*(1513), 37-49.

Routh, E. J. (1877). *A Treatise on the Stability of a Given State of Motion, Particularly Steady Motion: Being the Essay to which the Adams Prize was Adjudged in 1877, in the University of Cambridge*. Macmillan and Company.

Rynkiewicz, E. C., Pedersen, A. B., & Fenton, A. (2015). An ecosystem approach to understanding and managing within-host parasite community dynamics. *Trends in parasitology*, *31*(5), 212-221.

Scharsack, J. P., Franke, F., Erin, N. I., Kuske, A., Büscher, J., Stolz, H., ... & Kalbe, M. (2016). Effects of environmental variation on host–parasite interaction in three-spined sticklebacks (Gasterosteus aculeatus). *Zoology*, *119*(4), 375-383.

Susi, H., Barrès, B., Vale, P. F., & Laine, A. L. (2015). Co-infection alters population dynamics of infectious disease. Nature communications, 6(1), 1-8.

Van Leeuwen, A., Budischak, S. A., Graham, A. L., & Cressler, C. E. (2019). Parasite resource manipulation drives bimodal variation in infection duration. Proceedings of the Royal Society B, 286(1902), 20190456.

Verdy, A., & Amarasekare, P. (2010). Alternative stable states in communities with intraguild predation. Journal of Theoretical Biology, 262(1), 116-128.

Wodarz, D. (2006). Ecological and evolutionary principles in immunology. Ecology Letters, 9(6), 694-705.

Wolfram Research, Inc., Mathematica, Version 12.2, Champaign, IL (2020)

TABLES

Table 1. Equations for IGP (Eq. 1) and PIE models (PIE and PIEc constitutive immunity; Eq. 2) with top consumers (predators or immune cells), intermediate consumers (prey or parasite), and basal resource (or host energy). Listed below each model are the variables and parameters, their definition (with units), and corresponding default values used (in Figs. 3,4).

IGP	**PIE and PIEc**
$\frac{dP}{dt} = (e_{PN_1} f_{PN_1} N_1 + f_{PR} R - m_P) P$ (Eq. 1A)	$\frac{dI}{dt} = \frac{a_b E + e_{IN_1} f_{IN_1} N_1 EI}{e_I} - m_I I$ (Eq. 2A)
$\frac{dN_1}{dt} = (f_{N_1} R - f_{PN_1} P - m_N) N_1$ (Eq. 1B)	$\frac{dN_1}{dt} = \left(\frac{f_{N_1} E}{e_{N_1 E}} - f_{IN_1} I - m_N\right) N_1$ (Eq. 2B)
$\frac{dR}{dt} = a(S - R) - (f_{N_1} Q_{N_1} N_1 + f_{PR} Q_P P) R$ (Eq. 1C)	$\frac{dE}{dt} = \frac{f_E S}{h+S} - rE - (f_{N_1} N_1 E + e_{IN_1} f_{IN_1} N_1 I)E - a_b E$ (Eq. 2C)

Var	**Definition**	**Val. Fig. 3[a]**	**Val. Fig. 4[a]**	**Var**	**Definition**	**Val. Fig. 3**
P	Predator density (#·L^{-1})			I	Immune cell density (L^{-1})	
N_1	Prey density (#·L^{-1})			N_1	Parasite density (L^{-1})	
R	Resource density (#·L^{-1})			E	Host energy density (L^{-1})	
e_{PN_1}	Conversion, prey: predator	31.61	0.75	e_{IN_1}	Induction of energy per parasite killed by the immune response (L)	4
f_{PN_1}	Feeding rate, predator on prey, (L·day^{-1})	0.002	0.002	f_{IN_1}	Killing rate of parasite, per immune cell (L . time^{-1})	12
f_{PR}	Feeding rate, prey on resource (L . day^{-1})	0.0005	0.01	m_I	Immune cells background mortality rate (time^{-1})	24
m_P	Mortality rate, predator (day^{-1})	0.05	0.05	e_I	Cost of producing immune cell	3

f_{N_1}	Feeding rate, prey on resource (L·day^{-1})	var[b]	var[b]
m_N	Mortality rate, prey (day^{-1})	0.05	0.05
a	Dilution rate (day^{-1})	0.1	0.1
S	Supply point (L^{-1})	var[b]	var[b]
Q_P	Conversion, resource: predator	1	0.5
Q_{N_1}	Conversion resource: prey	1	2

e_{N_1E}	Cost of producing parasite	30
f_{N_1}	Feeding rate per parasite on energy (L . time^{-1})	var[b]
m_N	Mortality rate, parasite (time^{-1})	6
f_E	Host resource ingestion rate (L^{-1} . time^{-1})	44
S	Food supply point, hosts (L^{-1})	var[b]
h	Resource ingestion half-saturation constant, host (L^{-1})	19
r	Rate of host energy use for non-parasite purposes (time^{-1})	1
a_b	Baseline allocation to immunity (time^{-1})	PIE: 0 PIE$_c$: 0.03

[a] Values chosen in Fig. 3 such that $Q_{N_1} < e_{PN_1} Q_P$ (ensuring $F_3 < 0$; eqs. A14, 15). In fig. 4, $Q_{N_1} > e_{PN_1} Q_P$, enabling alternative stable states ($F_3 > 0$ for interior). [b] See values on figures.

Table 2. Equations for KP (Eq. 3) and 2PIE models (2PIE and 2PIEc constitutive immunity; Eq. 4) with top consumers (predators or immune cells), intermediate consumers (prey or parasites), and basal resource (or host energy). Listed below each model are the variables and parameters, their definition (with units), and corresponding default values used (in Figs. 6).

KP			**2PIE and 2PIEc**		
$\frac{dP}{dt} = (\Sigma e_{PN_i} f_{PN_i} N_i - m_P) P$ (Eq. 3A) $\frac{dN_i}{dt} = (e_{N_iR} f_{N_i} R - f_{PN_i} P - m_N) N_i$ (Eq. 3B) $\frac{dR}{dt} = a(S - R) - \Sigma(f_{N_i} N_i) Q R$ (Eq. 3C)			$\frac{dI}{dt} = \frac{a_b E + \Sigma e_{IN_i} f_{IN_i} N_i E I}{e_I} - m_I I$ (Eq. 4A) $\frac{d N_i}{dt} = \left(\frac{f_{N_i} E}{e_{N_iE}} - f_{IN_i} I - m_N\right) N_i$ (Eq. 4B) $\frac{dE}{dt} = \frac{f_E S}{h+S} - rE - (\Sigma e_{IN_i} f_{IN_i} N_i I + \Sigma f_{N_i} N_i) E - a_b E$ (Eq. 4C)		
Var	**Definition**	**Values Fig. 6[a]**	**Var**	**Definition**	**Values Fig. 6[a]**
P	Predator density (#·L^{-1})		I	Immune cells density (L^{-1})	
N_i	Prey *i* density (L^{-1})		N_i	Parasite *i* density (L^{-1})	
R	Resource density (L^{-1})		E	Host energy density (L^{-1})	
e_{PN_i}	Conversion, prey i: predator	2.4, 4.5	e_{IN_i}	Induced energy allocation rate per parasite *i* killed by the immune response (L)	3, 4.7
f_{PN_i}	Feeding rate, predator on prey *i*, (L·day^{-1})	9.8, 2.1	f_{IN_i}	Killing rate, immune cell on parasite *i* (L . time^{-1})	0.9, 0.4
e_{N_iR}	Conversion, resource: prey *i*	2.8, 2.8	m_I	Immune cells background mortality rate (time^{-1})	0.4
m_P	Mortality rate, predator (day^{-1})	0.1	e_I	Cost of producing immune cell	2.5

f_{N_i}	Feeding rate, prey on resource (L·day^{-1})	var[b], 10.4
m_N	Mortality rate, prey (day^{-1})[b]	0.1
a	Dilution rate (day^{-1})	7.9
S	Supply point (L^{-1})	var[b]
Q	Stoichiometric conversion, resource: prey	2.8[c]

e_{N_iE}	Cost of producing parasite *i*	4, 3.4
f_{N_i}	Feeding rate per parasite *i* on energy (L . time^{-1})	var[b], 7.2
m_N	Parasite background mortality rate (time^{-1})	0.8
f_E	Host resource ingestion rate L^{-1} . time^{-1})	7.8
S	Food supply point, hosts (L^{-1})	var[a]
h	Resource ingestion half-saturation constant (L^{-1})	3.2
r	Rate of host energy use for non-parasite purposes (time^{-1})	3.7
a_b	Baseline energy allocation to immunity (time^{-1})	2PIE: 0 2PIEc:0.1

[a] Values chosen to ensure N_1 is the superior competitor for resources without enemies (prey: $R_1^* < R_2^*$ [eq. A35]; parasite: $E_1^* < E_2^*$ [eq. A47.a]) while N_2 is more resistant to attack to enemies (prey: $f_{PN_1} > f_{PN_2}$; parasites: $f_{IN_1} > : f_{IN_2}$). Additionally, they guarantee the *effects on* ratio has structure $\alpha_1 > \alpha_2$ (eqs. A34, A46). [b] See values on figures. [c] Identical between prey i.

834 **FIGURE CAPTIONS**

835 **Figure 1**: *Direct interspecific effects and self-limitation in food web and within-host*
836 *parasite model*s. *Top row, single prey or parasite models (three-dimension, 3D)*: (A) one prey-
837 predator-resource (intraguild predation, IGP), (B) one parasite-immune cells-host energy (PIE),
838 and (C) PIEc with constitutive immunity (i.e., fixed allocation of energy to production of immune
839 cells). *Bottom row, two prey or two parasite models (four dimension, 4D):* (D) two prey - predator-
840 resource (keystone predation, KP), (E) two parasite - immune cells - host energy (2PIE), and (F)
841 2PIEc with constitutive immunity. All direct effects evaluated when densities are positive (i.e., at
842 a feasible interior equilibrium). Red (black) arrows: negative (positive) interspecific direct effect;
843 red curve: negative intraspecific specific effect.

844 **Figure 2:** *Intraspecific direct and indirect effects: an illustration of levels of feedback in*
845 *IGP, PIE, and PIEc models (Fig. 1A-C).* Evaluated at a feasible interior equilibrium, the IGP and
846 PIE models have similar feedback structure. PIEc adds additional loops involving immune self-
847 limitation. Level 1 feedback (F_1) is the sum of the shorter intraspecific direct effects (solid curves):
848 self-limitation (-) of resource/energy and immune cells (PIEc only). In intraspecific indirect effects
849 (dashed curves), each species limits or facilitates itself via interaction with other species in longer
850 loops. The intraspecific indirect effect (IE) sums that of energy, E (IE_E; yellow shading), parasite
851 N_1 (IE_{N_1}; blue), and immune cells I (IE_I; green). IE, in turn, is a ratio of two levels of feedback.
852 Level 2 feedback (F_2, numerator of IE) sums pairwise consumer-resource loops (-) and the product
853 of energy and immune self-limitation (-; only in PIEc; these are the numerators of the IE
854 components). Level 3 feedback (F_3, denominator of IE) sums three-species loops. These loops
855 from *L-R* are: (i) "N_1 *is eaten*", the I-N_1 loop times E self-limitation (-), (ii) "*starving the enemy*"
856 (+), (iii) "*feeding the enemy*" (-), and (iv) "N_1 *eats*", the E- N_1 loop times I self-limitation (- ; PIEc
857 only). This sum of (i)-(iv) determines the sign of F_3 and of IE (since IE = $-F_2/F_3$, and $F_2 < 0$
858 always). The predator (P, green), prey (N_1, blue), and resources (R, yellow) in IGP are analogous

859 to immune cells (I), parasite (N_1), and host energy (E), respectively, in the PIE models.

860 **Figure 3:** *Weakening of the product of intraspecific direct and indirect effects generates*
861 *oscillations in both IGP and PIE / PIEc models (Fig. 1, Box 1).* (A)-(C) *Bifurcation diagrams* over
862 gradients of supply point (S) and feeding rate of prey or parasite (f_{N_1}): Oscillations (dark orange
863 region) found in (A) IGP also arise in (B) PIE models of within-host dynamics (see Appendix
864 Section 2). These oscillatory regions are enveloped within a region of stable coexistence (light
865 orange). In PIE models, a_b denotes baseline energy allocated to immune cells: $a_b > 0$ in (C) PIEc.
866 (D)-(F) *Direct and indirect effects (after Fig. 2)*: Oscillations occur with weakening of the product
867 of intraspecific direct effects (DE) and intraspecific indirect effects (IE). Weakening of IE
868 primarily triggers oscillations at low f_{N_1} while strengthening of DE restores stability at higher f_{N_1}
869 in (D) IGP and (E) PIE. In (F) PIEc, self-limitation comes from energy (DE_E, orange) and immune
870 cells (DE_I, green). Summed DE eliminates oscillations while lowering parasite burden relative to
871 PIE (see also Fig. A2). (G)-(I) *Equilibrial densities along* f_{N_1}: resource, R^* or energy, E^* (orange);
872 prey or parasite, N_1^*, (blue); and predator, P^* or immune cells, I^* (green) in (G) IGP, (H) PIE, and
873 (I) PIEc models. Shifts in these densities weakens or strengthens DE and IE (see text and Appendix
874 Section 2 for details; Table 1 for default parameters).

875 **Figure 4***: Positive intraspecific indirect feedback leads to two forms of alternate stable*
876 *states (Alt SS-1 and -2) in the IGP model of prey (N_1), predators (P), and resources (R) not found*
877 *in PIE models.* (A) A bifurcation diagram over gradients of resource supply point (S) and prey
878 feeding rate (f_{N_1}) and species dynamics at the interior equilibrium (see Fig. A2 for more details).
879 (B-D) Sample dynamics. (A,B) Stable coexistence ($R - N_1 - P$, light orange) found in IGP also
880 arises in PIE predicting successful infection (Fig 3; $E - N_1 - I$). (B-D) IGP predicts two forms of
881 alternate stable states, where initial densities (inset) determine competitive outcomes between N_1
882 and P. (A, C): In more typical alternative stable states (Alt SS-1; dark grey), either prey (R-N_1) or
883 predator (R-P) wins. Analogous within-host states would lead to infection (E-N_1) or not (E-I). (A,

884 F) Another example (Alt SS – 2; light grey) predicts either coexistence (R-N_1-P) or an only-
885 predator (R-P) equilibrium (analogous to infection [E-N_1-I] or clearance [E-I]). Neither of these
886 types of alternative states emerge in PIE models (see text, Appendix Section 2).

887 **Figure 5**: *Intraspecific direct and indirect effects in four-dimension models: feedback in*
888 *KP, PIE, and 2PIEc (Fig 1).* Evaluated at a feasible interior equilibrium, feedbacks for KP and
889 2PIE are nested within 2PIEc. In 2PIE and 2PIEc, additional loops arise from interactions between
890 immune cells and host energy ("add loop in 2PIE & 2PIEc"), and immune self-limitation loop
891 ("add loop in 2PIEc"). Level 1 feedback (F_1) sums intraspecific direct effects (solid curves) from
892 energy and immune self-limitation (- ; only in 2PIEc). The intraspecific indirect effects (dashed
893 curves) involve a ratio of longer loops, where each species, N_1 ($\mathrm{IE}_{\mathrm{N}_1}$; blue shading) and N_2
894 ($\mathrm{IE}_{\mathrm{N}_2}$; purple shading), interacts with others in feedback at level 3 (F_3) and 4 (F_4). F_3 sums three
895 species loops in PIE models: (i) "N_1 *is eaten*", the I-N_1 loop times E self-limitation (- ; all models),
896 (ii) "*starving the enemy*" (+ ; from PIE models), (iii) "*feeding the enemy*" (-; from PIE models),
897 and (iv) "N_1 *eats*", the E-N_1 loop times I self-limitation (- ; only from PIEc). F_4 sums, from L-R,
898 two destabilizing (+) loops and stabilizing (-) ones. N_i benefits as it (i) "*feeds*" or (ii) "*starves*" the
899 enemy, but is restrained by (iii) and (iv) "N_i *is eaten,* N_j *eats*" loops (the product of I-N_i and N_j-E
900 loops). With some rearrangement, F_4 becomes proportional to differences in ratios of how each
901 competitor has *effects on* ($\varepsilon_1 - \varepsilon_2$) and is *affected by* ($\alpha_1 - \alpha_2$) immune cells and host energy (see
902 text). Finally, the sign of F_4 determines that of IE (see text). The predator (P, green), prey 1 (N_1,
903 blue), prey 2 (N_2, purple), and resources (R, yellow) in KP are analogous to immune cells (I),
904 parasites (N_1 and N_2), and host energy (E) in 2PIE models, respectively.

905 **Figure 6**: *KP anticipates coexistence and alternate stable states in 2PIE models.* (A)-(C).
906 *Bifurcation diagrams* over gradients of resource supply point (S) and feeding rate of prey or
907 parasite (f_{N_1}): alternative stable states or priority effects (grey region) and stable coexistence
908 (orange) found in (A) KP also arise in (B) 2PIE and (C) 2PIE constitutive immunity (2PIEc)

models of within-host dynamics. In 2PIE, a_b denotes baseline energy allocated to immune cells. Stable coexistence (coinfection) happens at low f_{N_1} and S in all models. (D)-(F) *Indirect effects through coexistence/coinfection regions*: Strong, negative indirect effects (IE; black, short dash) from N_1 ($\mathrm{IE}_{\mathrm{N}_1}$; blue, long dash) and N_2 ($\mathrm{IE}_{\mathrm{N}_2}$; purple, long dash) shift systems from coexistence to exclusion of N_1 or N_2 at lower or higher f_{N_1} respectively in (D) KP, (E) 2PIE, and (F) 2PIEc. (F) Immune self-limitation in 2PIEc enhances negative indirect effects and squeezes parameter space enabling coinfection. (G)-(I) *Equilibrial densities along* f_{N_1}: Resource, R or energy, E (orange); prey or parasite 1, N_1, (blue); prey or parasite 2, N_2, (purple); and predator, P or immune cells, I (green) in (G) KP, (H) 2PIE, and (I) 2PIEc models. (See text and Appendix Section 3 for details, Table 2 for default parameters).

Box 1. *A feedback loop approach to analyze a general 3-dimensional system of equations*

Imagine three species N_1, N_2 and N_3 where the effects of their interactions are captured by a 3D Jacobian matrix (J_3):

$$J_3 = \begin{bmatrix} J_{11} & J_{12} & J_{13} \\ J_{21} & J_{22} & J_{23} \\ J_{31} & J_{32} & J_{33} \end{bmatrix}$$

Characteristic polynomial of J_3

$$\lambda^3 + \lambda^2 F_1 + \lambda F_2 + F_3$$

F_i is level of feedback

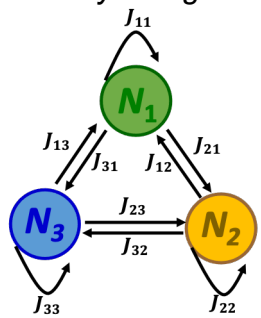

Stability requires that ..

$F_1 < 0$
$F_2 < 0$
$F_3 < 0$

.. each level of feedback is negative*

and $F_1 F_2 + F_3 > 0$

We rewrite this criterion as $F_1 \times \left(-\frac{F_2}{F_3}\right) > 1$ to highlight intraspecific direct and indirect effects

Stability as a product of intraspecific direct effects (DE) and indirect effects (IE) (Appendix)

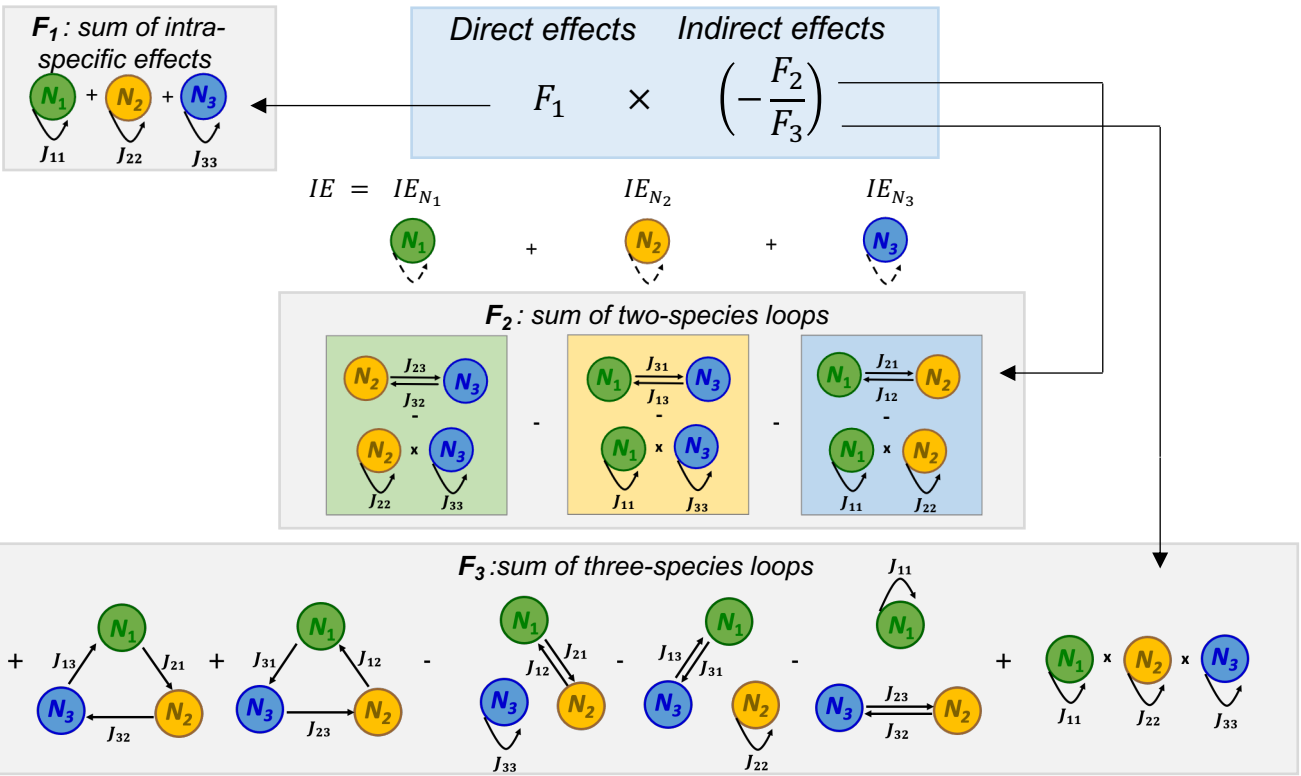

Stability of an equilibrium depends on the sign and strength of the product of DE and IE

Alternate stable states:
Indirect effects are positive (DE < 0, IE > 0)

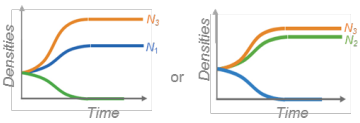

Stable coexistence:
Direct and indirect effects are negative (DE < 0, IE < 0) and jointly strong (DE x IE > 1)

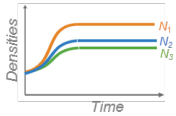

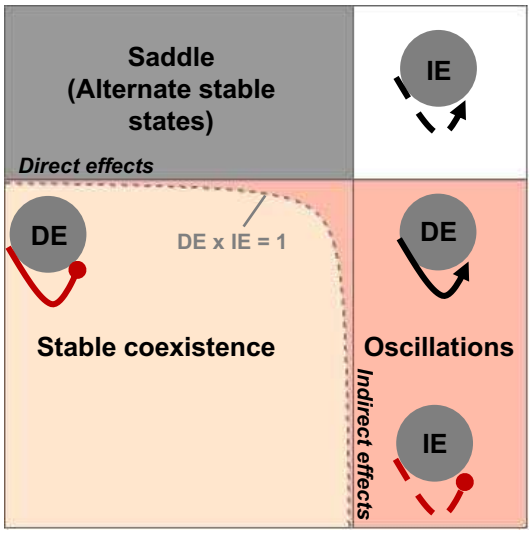

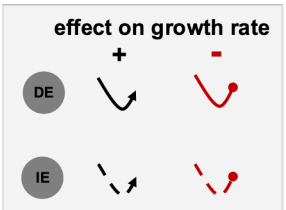

Oscillations:
Weakening of DE x IE
1.DE < 0 and IE < 0, DE x IE < 1
2.DE > 0 and IE < 0.

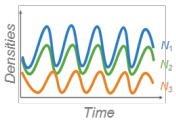

*Note: The signs required for stability using Routh Hurwitz criteria (more traditional) are opposite those here for feedback. Thus, F_1 is Tr($\mathbf{J_3}$) and F_3 is -|$\mathbf{J_3}$|

Figure 1

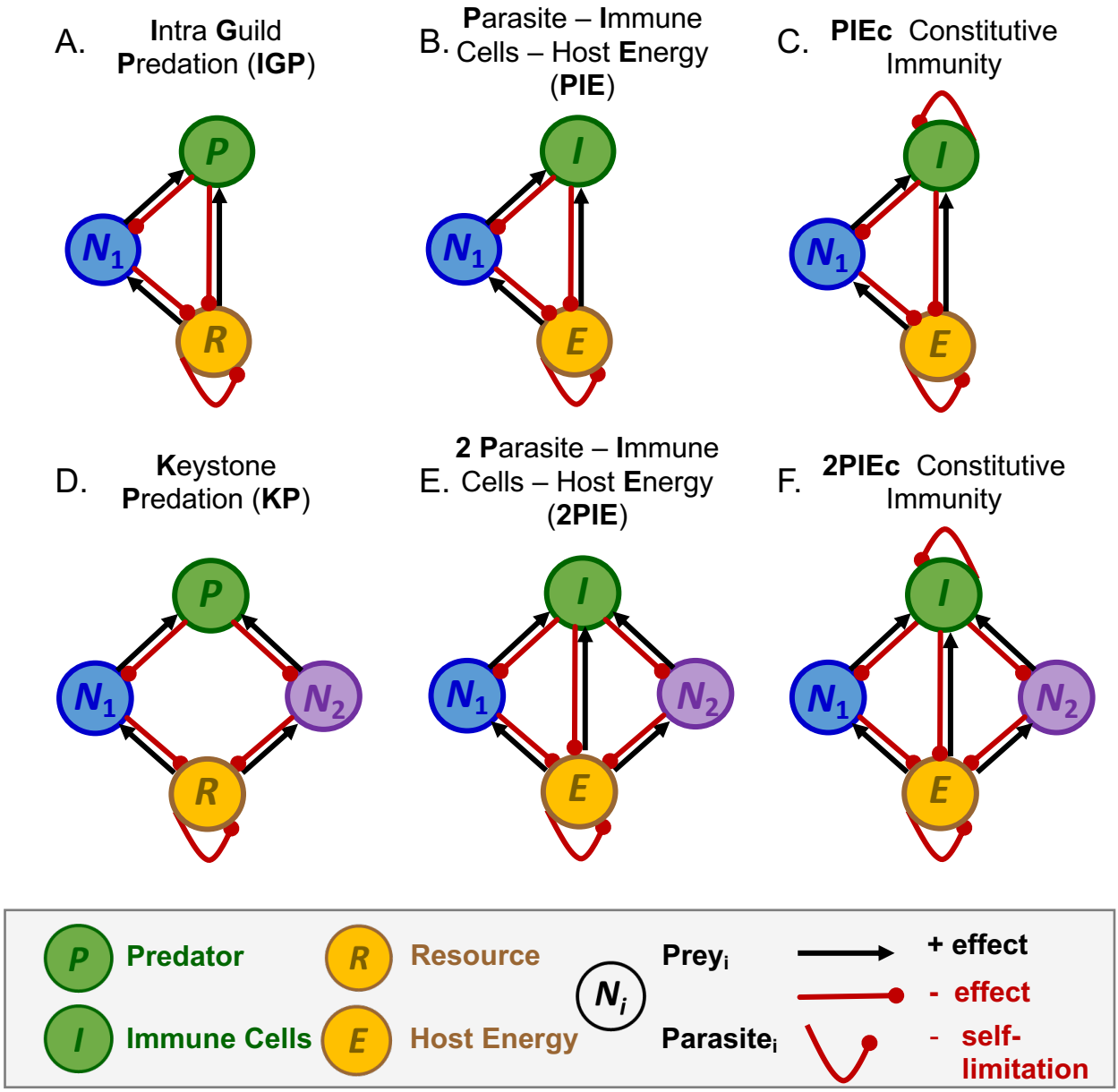
A.
Intra Guild Predation (IGP)
B.
Parasite – Immune Cells – Host Energy (PIE)
C.
PIEc Constitutive Immunity
D.
Keystone Predation (KP)
E.
2 Parasite – Immune Cells – Host Energy (2PIE)
F.
2PIEc Constitutive Immunity
P
I
N1
N2
R
E
Predator
Immune Cells
Resource
Host Energy
Ni
Preyi
Parasitei
+ effect
- effect
- self-limitation

Figure 2

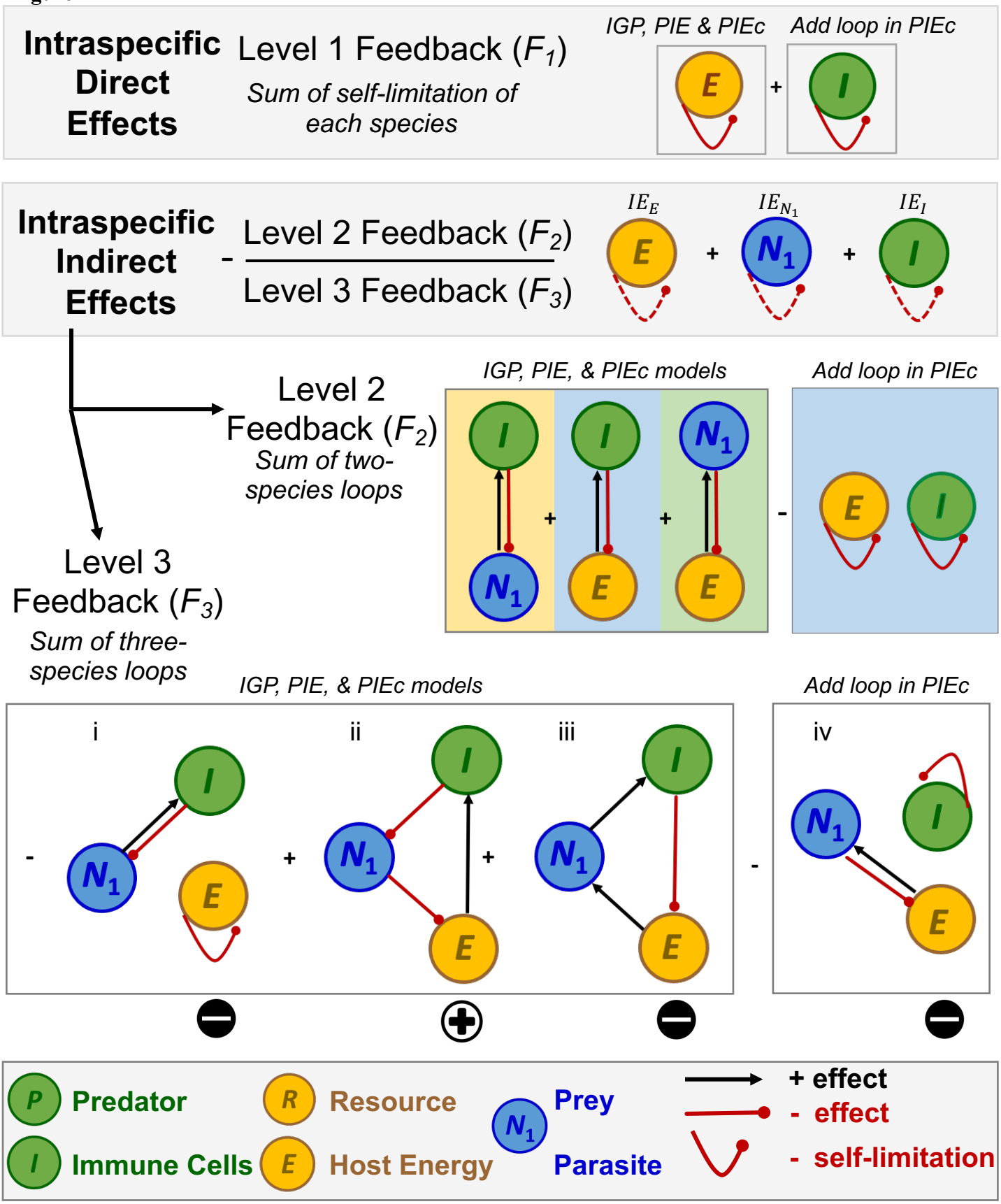
Intraspecific Direct Effects
Level 1 Feedback (F_1)
Sum of self-limitation of each species
IGP, PIE & PIEc
Add loop in PIEc
Intraspecific Indirect Effects
Level 2 Feedback (F_2)
Level 3 Feedback (F_3)
IE_E
IE_{N_1}
IE_I
Level 2 Feedback (F_2)
Sum of two-species loops
IGP, PIE, & PIEc models
Add loop in PIEc
Level 3 Feedback (F_3)
Sum of three-species loops
IGP, PIE, & PIEc models
Add loop in PIEc
i
ii
iii
iv
Predator
Immune Cells
Resource
Host Energy
Prey
Parasite
+ effect
- effect
- self-limitation

Figure 3

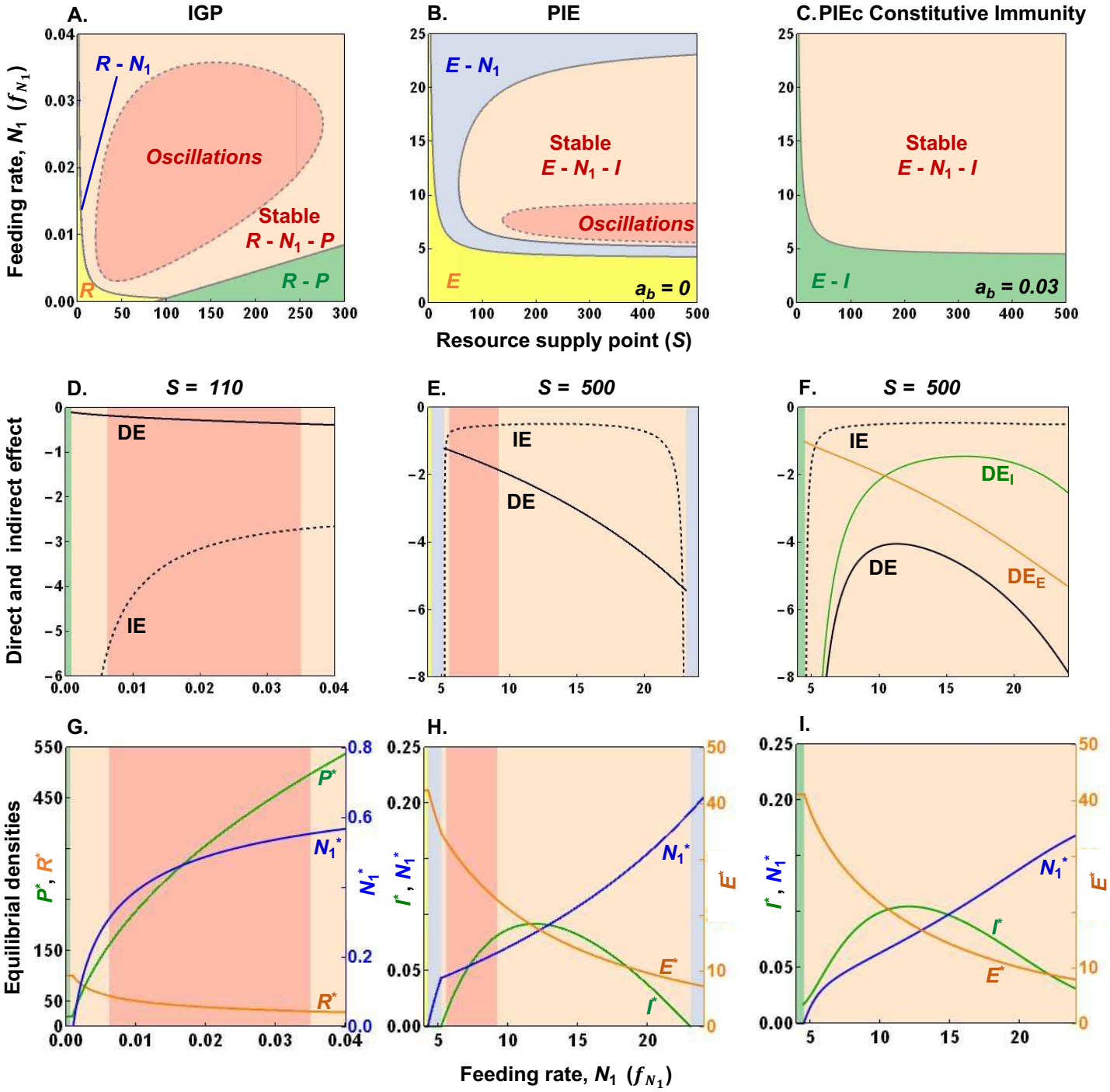
A. IGP
B. PIE
C. PIEc Constitutive Immunity
Feeding rate, N_1 (f_{N_1})
R - N_1
Oscillations
Stable
R - N_1 - P
R - P
R
E - N_1
Stable
E - N_1 - I
Oscillations
E
a_b = 0
Stable
E - N_1 - I
E - I
a_b = 0.03
Resource supply point (S)
D. S = 110
E. S = 500
F. S = 500
Direct and indirect effect
DE
IE
IE
DE
IE
DE_I
DE
DE_E
G.
H.
I.
Equilibrial densities
P^*, R^*
N_1^*
P^*
N_1^*
R^*
I^*, N_1^*
E^*
N_1^*
E^*
I^*
I^*, N_1^*
E^*
N_1^*
I^*
E^*
Feeding rate, N_1 (f_{N_1})

Figure 4

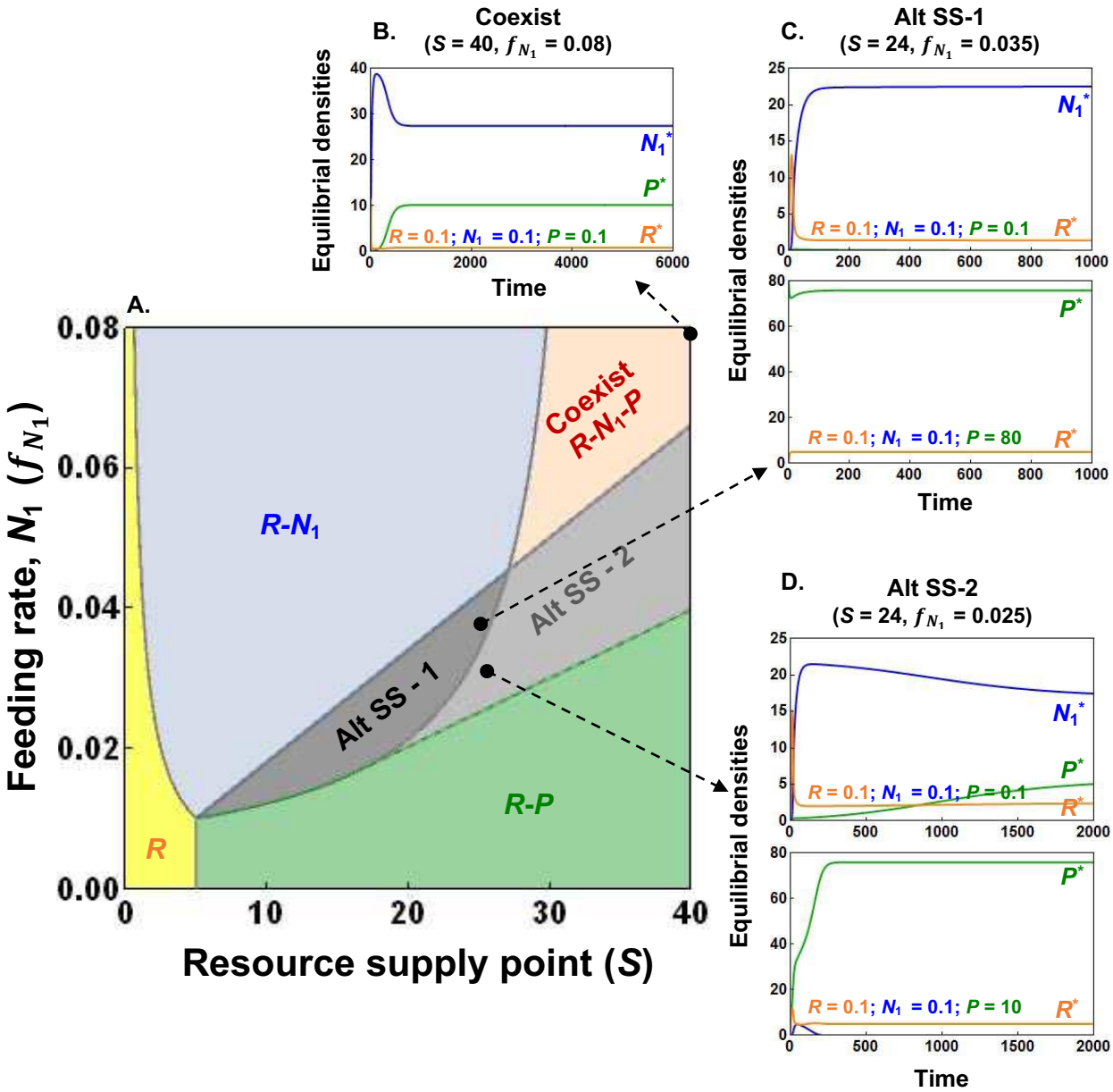
A.
B.
Coexist
(S = 40, f_{N_1} = 0.08)
C.
Alt SS-1
(S = 24, f_{N_1} = 0.035)
D.
Alt SS-2
(S = 24, f_{N_1} = 0.025)
Equilibrial densities
Time
Feeding rate, N_1 (f_{N_1})
Resource supply point (S)
R-N_1
Coexist R-N_1-P
Alt SS - 1
Alt SS - 2
R-P
R
N_1^*
P^*
R^*
R = 0.1; N_1 = 0.1; P = 0.1
R = 0.1; N_1 = 0.1; P = 80
R = 0.1; N_1 = 0.1; P = 10

Figure 5

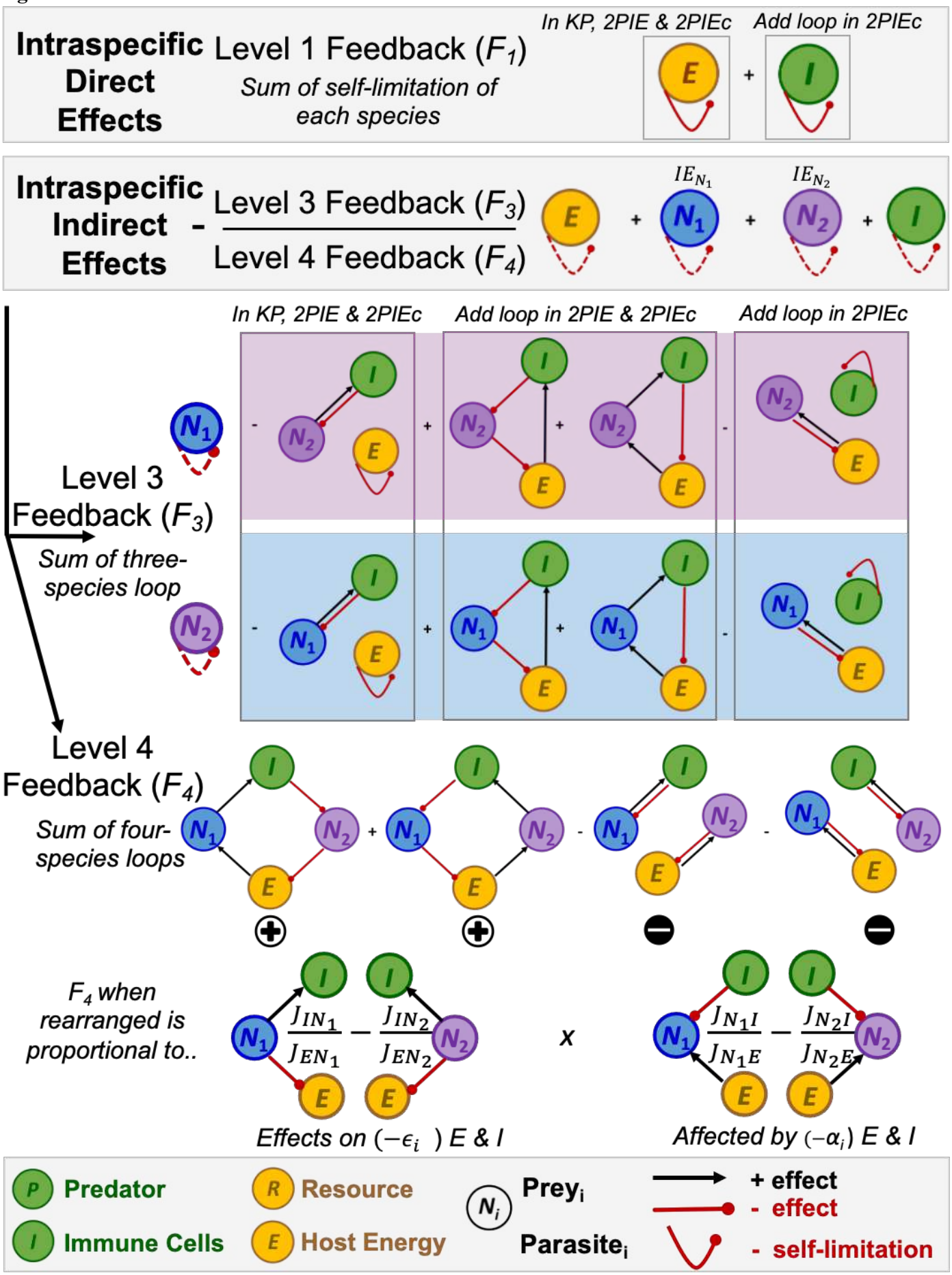
Intraspecific Direct Effects
Level 1 Feedback (F_1)
Sum of self-limitation of each species
In KP, 2PIE & 2PIEc
Add loop in 2PIEc
Intraspecific Indirect Effects
Level 3 Feedback (F_3)
Level 4 Feedback (F_4)
IE_{N_1}
IE_{N_2}
In KP, 2PIE & 2PIEc
Add loop in 2PIE & 2PIEc
Add loop in 2PIEc
Level 3 Feedback (F_3)
Sum of three-species loop
Level 4 Feedback (F_4)
Sum of four-species loops
F_4 when rearranged is proportional to..
$\frac{J_{IN_1}}{J_{EN_1}} - \frac{J_{IN_2}}{J_{EN_2}}$
x
$\frac{J_{N_1I}}{J_{N_1E}} - \frac{J_{N_2I}}{J_{N_2E}}$
Effects on ($-\epsilon_i$) E & I
Affected by ($-\alpha_i$) E & I
Predator
Immune Cells
Resource
Host Energy
Prey$_i$
Parasite$_i$
+ effect
- effect
- self-limitation

Figure 6

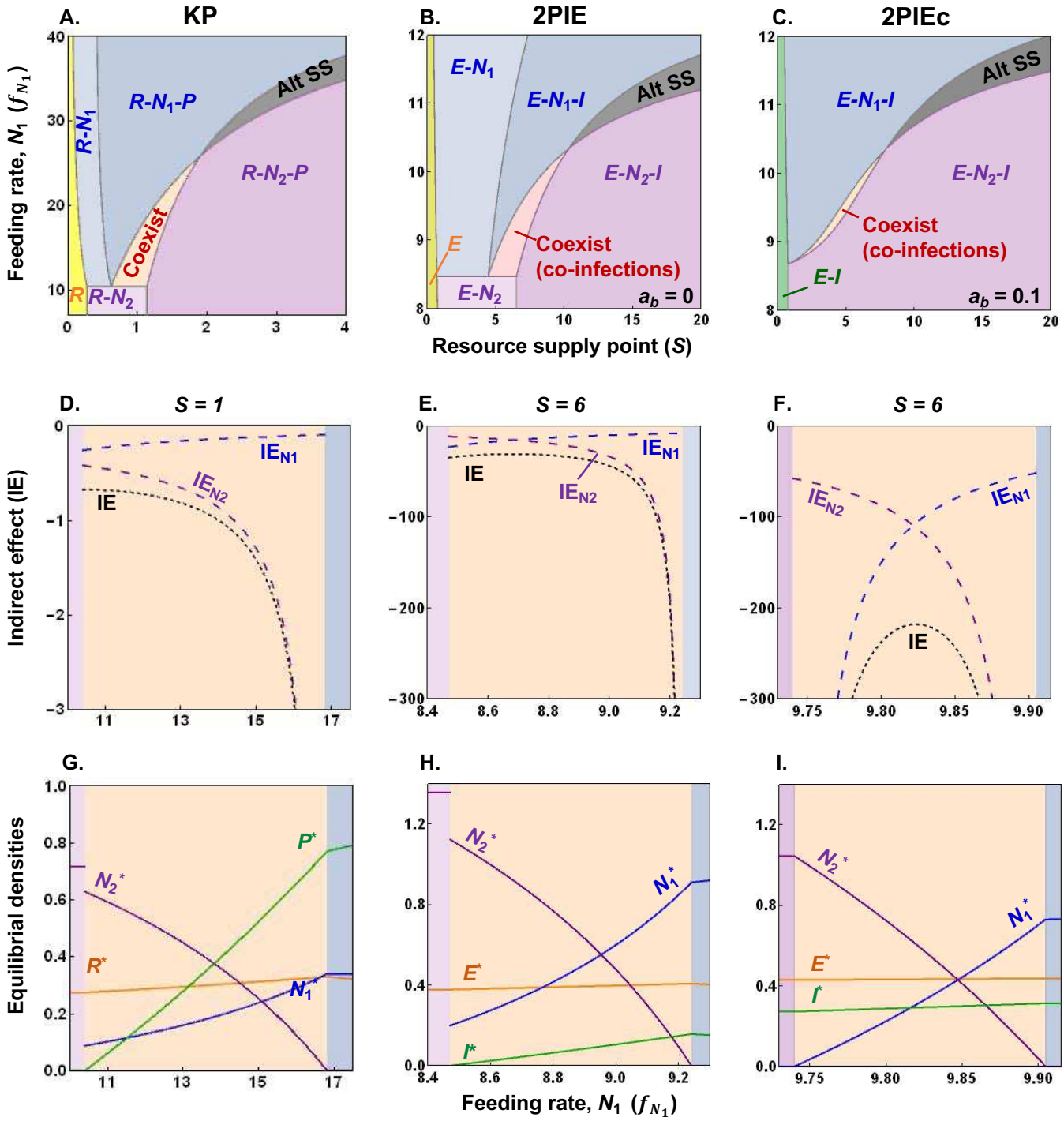
A.
KP
B.
2PIE
C.
2PIEc
Feeding rate, N_1 (f_{N_1})
R-N1
R-N1-P
Alt SS
R-N2-P
Coexist
R
R-N2
E-N1
E-N1-I
E-N2-I
E
E-N2
Coexist
(co-infections)
ab = 0
E-I
ab = 0.1
Resource supply point (S)
D.
S = 1
E.
S = 6
F.
S = 6
Indirect effect (IE)
IEN1
IEN2
IE
G.
H.
I.
Equilibrial densities
N2*
P*
R*
N1*
E*
I*
Feeding rate, N_1 (f_{N_1})